

# DNA-Driven Dynamic Assembly/Disassembly of Inorganic Nanocrystals for Biomedical Imaging

Shengfei Yang,<sup>#</sup> Yuqi Wang,<sup>#</sup> Qiyue Wang,<sup>#</sup> Fangyuan Li,<sup>\*†</sup> and Daishun Ling<sup>\*</sup>

 Cite This: *Chem. Biomed. Imaging* 2023, 1, 340–355

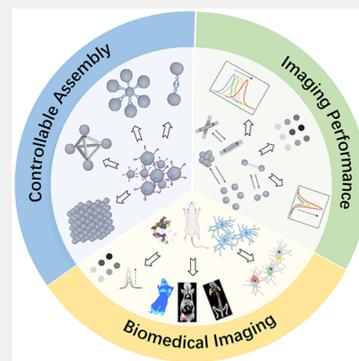
 Read Online

ACCESS |

 Metrics & More

 Article Recommendations

**ABSTRACT:** DNA-mediated programming is emerging as an effective technology that enables controlled dynamic assembly/disassembly of inorganic nanocrystals (NC) with precise numbers and spatial locations for biomedical imaging applications. In this review, we will begin with a brief overview of the rules of NC dynamic assembly driven by DNA ligands, and the research progress on the relationship between NC assembly modes and their biomedical imaging performance. Then, we will give examples on how the driven program is designed by different interactions through the configuration switching of DNA-NC conjugates for biomedical applications. Finally, we will conclude with the current challenges and future perspectives of this emerging field. Hopefully, this review will deepen our knowledge on the DNA-guided precise assembly of NCs, which may further inspire the future development of smart chemical imaging devices and high-performance biomedical imaging probes.



**KEYWORDS:** DNA nanotechnology, programmable materials, self-assembly, dynamic assembly, responsive materials, DNA probe, bioimaging, biomedical diagnosis

## 1. INTRODUCTION

Nano- and microstructures influence the physical properties of matter.<sup>1</sup> In particular for inorganic nanocrystals (NCs),<sup>2,3</sup> various unexpected properties have been explored, including in photonics,<sup>4,5</sup> thermoelectrics,<sup>6,7</sup> and magnetism.<sup>8–10</sup> Surface ligands play a crucial role in regulating the assembly and disassembly of NCs, controlling their structures and functions at multiscales,<sup>11,12</sup> and making them a strong candidate for the development of cutting-edge next-generation imaging probes. As a typical example, controlling the assembly structures of plasmonic NCs to modulate their plasmonic resonance properties has been widely exploited to construct functional nanoarchitectures for biosensors and optical analysis systems during the past decades,<sup>13–21</sup> in which the precise assembly of NCs is the key to elaborate and verify plasmonic coupling effects.<sup>20–22</sup>

By tuning the various assembly/disassembly parameters, including the change of interparticle spacing, aggregation state, arrangement direction, and assembly composition, the properties of NCs can be regulated to suit a given bioimaging application.<sup>23–28</sup> However, it is difficult to predict the organization and structure of nanoscale assembly due to the lack of interaction with sufficient directionality for driving NCs.<sup>29</sup> In the past four decades, with the vigorous development of DNA nanotechnology, DNA-mediated self-assembly has been developed as an effective approach to prepare highly programmable nanostructures with controllable size and shape,<sup>30–34</sup> which provides a promising methodology for

driving the precise assembly of NCs via the directional base pairing.<sup>35</sup> Specifically, Watson–Crick base-pairing interactions (A–T and G–C) define DNA directionality, and varying base amounts and sequences can program the geometry of DNA nanoassembly.<sup>36,37</sup> Programmable DNAs are modified on the surface of NCs and drive their directional movement, hence manipulating the dynamic assembly of NCs.<sup>38–43</sup> In addition to base complementarity, DNA possesses a variety of unique biological and chemical features. For example, the designed DNA sequences can develop a specific secondary structure and switch their configuration under the interaction of metal ions,<sup>44,45</sup> small molecules,<sup>46,47</sup> and proteins.<sup>47,48</sup> Once stimulated, the switchable DNA structures can act as procedures to drive dynamic assembly/disassembly of NCs for changing the imaging performance of NCs, resulting in responsive signals. These elegant characteristics indicate that DNA is a reliable baseband for NCs to realize efficient biomedical imaging.<sup>49–52</sup>

In this review, the design principle and biomedical imaging applications of DNA-driven dynamic NC assemblies are summarized (Figure 1). First, we briefly discuss the

**Received:** February 15, 2023

**Revised:** March 20, 2023

**Accepted:** April 7, 2023

**Published:** May 8, 2023



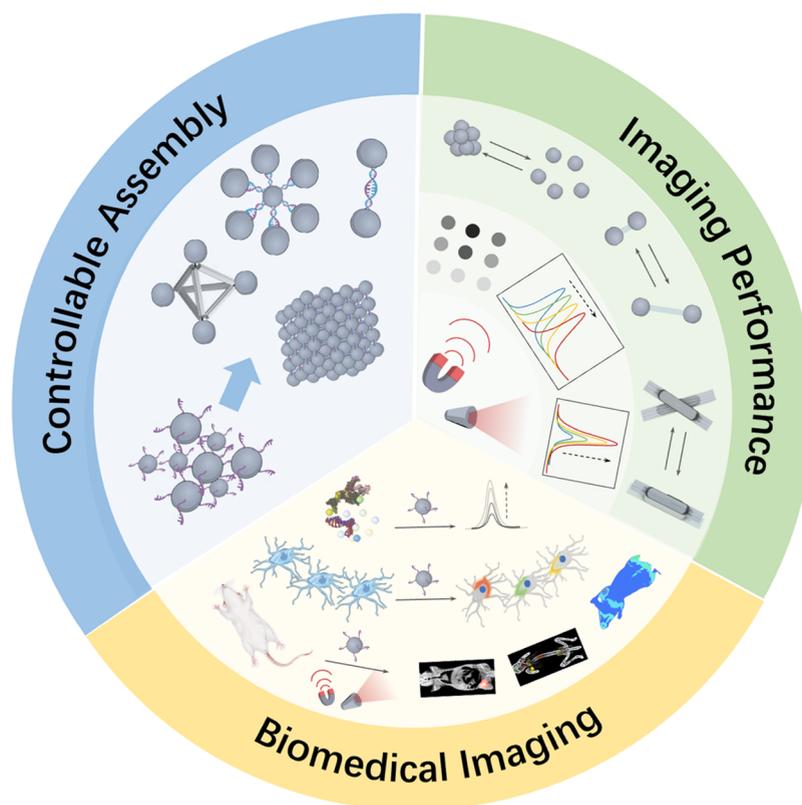


**Figure 1.** Schematic illustration of DNA-driven dynamic assembly/disassembly of NCs for biomedical imaging.

fundamental mechanisms of DNA-mediated NC assemblies and their regulated imaging properties. Then, the biomedical imaging applications using DNA-driven dynamic NC assemblies are reviewed. Finally, the challenges and perspectives in the biomedical applications of DNA-mediated dynamic NC assemblies are discussed.

## 2. CONTROLLABLE ASSEMBLY OF NCs

Controlling the placement of each component is absolutely a grand challenge to construct materials and tailor their properties for a given application. The interaction with sufficient directionality to accurately predict the final arrangement and orientation of components is highly important for controlled NC assembly.<sup>29</sup> As a storage material for genetic information, DNA strictly follows the Watson–Crick hydrogen-bonding rules, which are able to control the hybridization of DNA strands with high selectivity and specificity by permuting the nucleobase sequence of DNA strands and assemble nanostructures via “bottom-up” strategies.<sup>53–55</sup> Since Mirkin’s and Alivisatos’s groups demonstrated the powerful methodology of DNA-guided NC self-assembly in 1996,<sup>56,57</sup> the field of material engineering based on the assembly of homogeneous and heterogeneous NCs’ crystal structures has been developed rapidly.<sup>58,59</sup> The DNA-guided NC self-assembly methodology developed into two branches: “NCs template-assisted assembly” and “DNA template-assisted assembly”. In brief, the former strategy developed by the Mirkin group describes that DNA mainly acts as connectors, driving assembly and determining the spacing of NCs, in which the assembly orientation and arrangement pattern are dominated by the geometric characteristics of NCs.<sup>29</sup> For the second strategy, a discrete number of DNA strands can guide the NCs’ directional assembly. Therefore, DNA not only

cross-links the NCs, but also acts as a template to determine the arrangement direction and structural pattern of the NCs.<sup>60</sup>

NCs as the template can be directionally assembled and programmed by the interaction forces of DNAs, analogous to atomic assembly manipulated by covalent bonds.<sup>29,61–64</sup> The NCs modified with dense DNA ligands can act as programmable atom equivalents (PAEs), and DNA hybridization plays a role in controlling nanomodule construction as the “value” and “bond” (Figure 2A).<sup>65–67</sup> Similar to the chemical bonds that control the arrangement of atoms in an ordered crystal structure, the DNA “bond” can also drive NCs to form various three-dimensional superlattices.<sup>40,68–70</sup> By regulating the length or sequence of DNA and the size of PAEs, NCs can be precisely positioned into a variety of crystal structures.<sup>40</sup> It is always the most stable state that maximizes the number of “bonds” formed by DNA hybridization in a lattice arrangement, in which the surface-area contact between NCs bearing complementary linkers can be used as a proxy for counting the hybridization events.<sup>29,40</sup> For instance, as shown in Figure 2B: (i) Sharing a single self-complementary DNA sequence that allows all PAEs to bond equivalently, face-centered cubic (FCC) crystal assembly maximizes the total number of closest neighbors for each NC within a lattice. (ii) Two different sequences as termini on DNA bonds can hybridize with each other (nonself-complementary) and assemble NCs with a body-centered cubic (BCC) crystal structure. (iii) Tuning the hydrodynamic radii of PAEs that are determined by NCs size and DNA length, NCs can be positioned within a given unit cell of lattice type to form a variety of crystallographic symmetry such as AIB2 crystals.

It is crucial to note that the general method is advantageous for assembling various types of NCs, which examine the effect of the spatial arrangement of NCs with different chemical

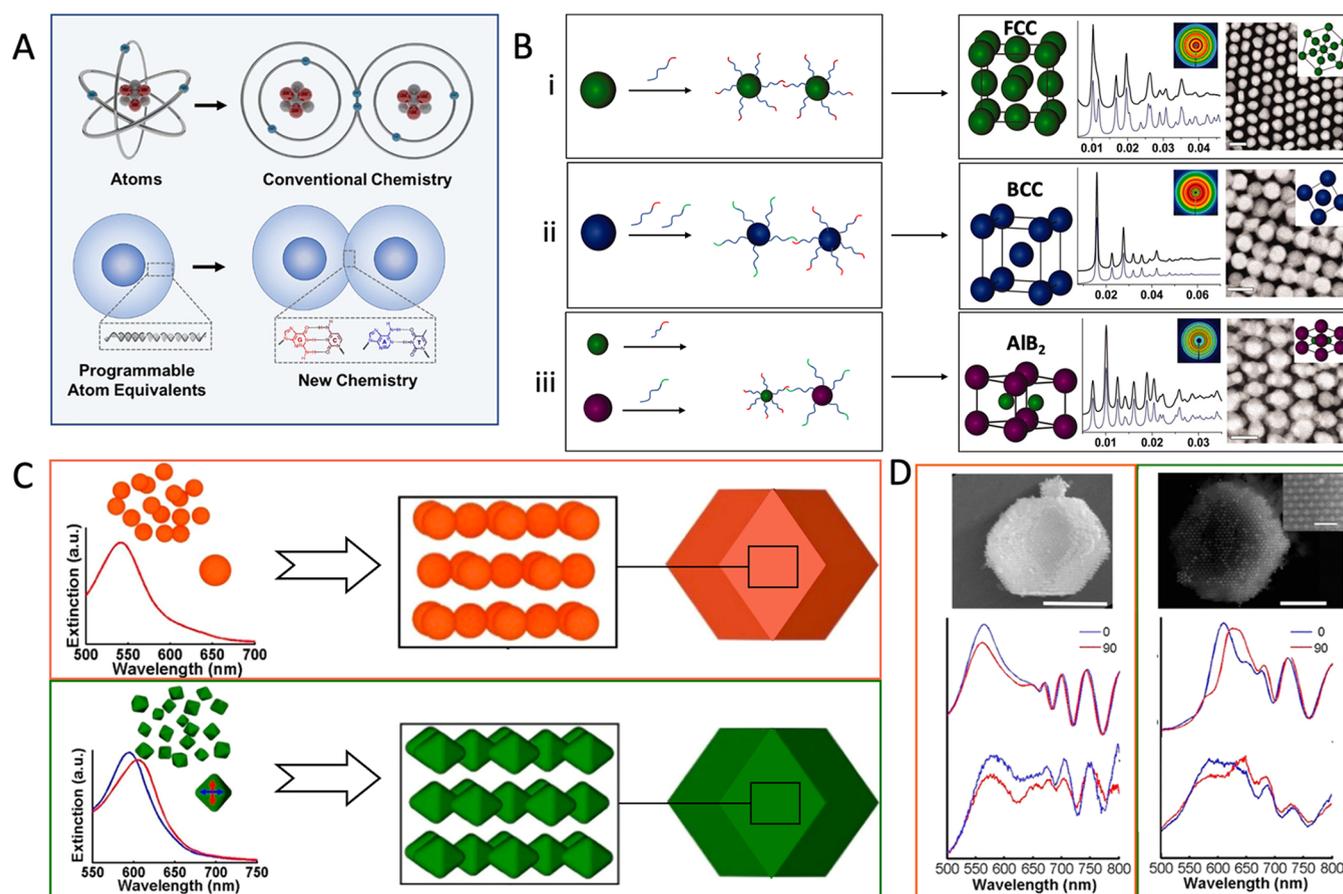


**Figure 2.** (A) Schematic illustration of DNA-NC conjugates acting as programmable atom equivalents (PAEs) for bonding assembly in a manner analogous to a natural atom assembly system. Reproduced with permission from ref 65. Copyright (2021) American Chemical Society. (B) DNA-mediated FCC (i), BCC (ii), AlB<sub>2</sub> (iii) superlattice assembly of NCs; each panel contains a model unit cell, 1D and 2D (inset) X-ray diffraction patterns, and a TEM image. Reproduced with permission from ref 40. Copyright (2011) The American Association for the Advancement of Science. (C) The schematic depiction and single nanoparticle extinction spectra of the superlattices made from either octahedral (green) or spherical (orange) NCs. (D) SEM image and backscattering spectra of (C). Reproduced with permission from ref 76. Copyright (2017) American Chemical Society.

compositions,<sup>71,72</sup> sizes,<sup>71</sup> or shapes<sup>73,74</sup> on their macro-properties.<sup>65</sup> For example, by controlling the crystal habit of plasmonic NCs superlattices assembled by DNA sequence, Mirkin et al. illustrated how DNA-mediated NC assembly controls light confinement and far-field extinction in plasmonic assembly through the optical responsiveness, which is demonstrated by both experiments and electrodynamic simulations.<sup>75</sup> Meanwhile, the three-dimensional lattice assembled from octahedral NCs exhibits a unique polarization-dependent optical responsiveness different from spherical NCs, as determined by finite-difference time-domain simulations and backscattering measurements (Figure 2C,D), which indicates that the incorporation of anisotropic NCs contributes to expanding the diversity of programmable NC assemblies for optical tools.<sup>76</sup> Furthermore, Mirkin and Cruz's group first discovered that the small DNA-NC conjugates with electronic-like properties can act as electronic equivalents (EEs) to stabilize the larger PAEs and diffuse within the lattice, analogous to the metallic bonding.<sup>77–80</sup> Thus, the introduction of EEs provides an assembly method to break the high symmetry of NCs superlattice: the DNA as valence bond connected to NCs is not necessarily completely fixed in space and no longer restricts NC assembly on a single cell.<sup>77–80</sup> Based on this concept, a series of crystal structures were

successfully constructed, and the electron microscopy results and molecular dynamics simulation clearly demonstrated that the DNA-driven NC assembly can generate lower symmetrical crystal structures and even create unexpected lattice arrangements.<sup>77</sup> Such a programmable assembly approach indicates that the diverse properties of nanomaterials can be regulated by both the length of DNA and the geometric configuration of NC, which facilitates the elucidation of the relationship between the assembly parameter and performance of NCs and will guide the development of biomedical imaging nanoplatforms.

On the other hand, the hybridization of stands is able to create rigid structures that can be used as a template to precisely locate NCs. In the DNA template assembly strategy, DNA modified on the surface drives NC to be arranged at the predetermined position of the template, instead of cross-linking between NCs, achieving the nanoscale patterning with precise spatial location and number of NCs.<sup>81–86</sup> Differing from the NCs template-assisted assembly, the arrangement of NC is determined by the geometry of the DNA pattern. Moreover, the development of advanced DNA nanostructures has given a new opportunity for DNA template-based NCs-assembly (such as DNA tiles<sup>87–89</sup> and DNA origami<sup>32,90,91</sup>). As shown in Figure 3A, the rigidity of DNA structure provides

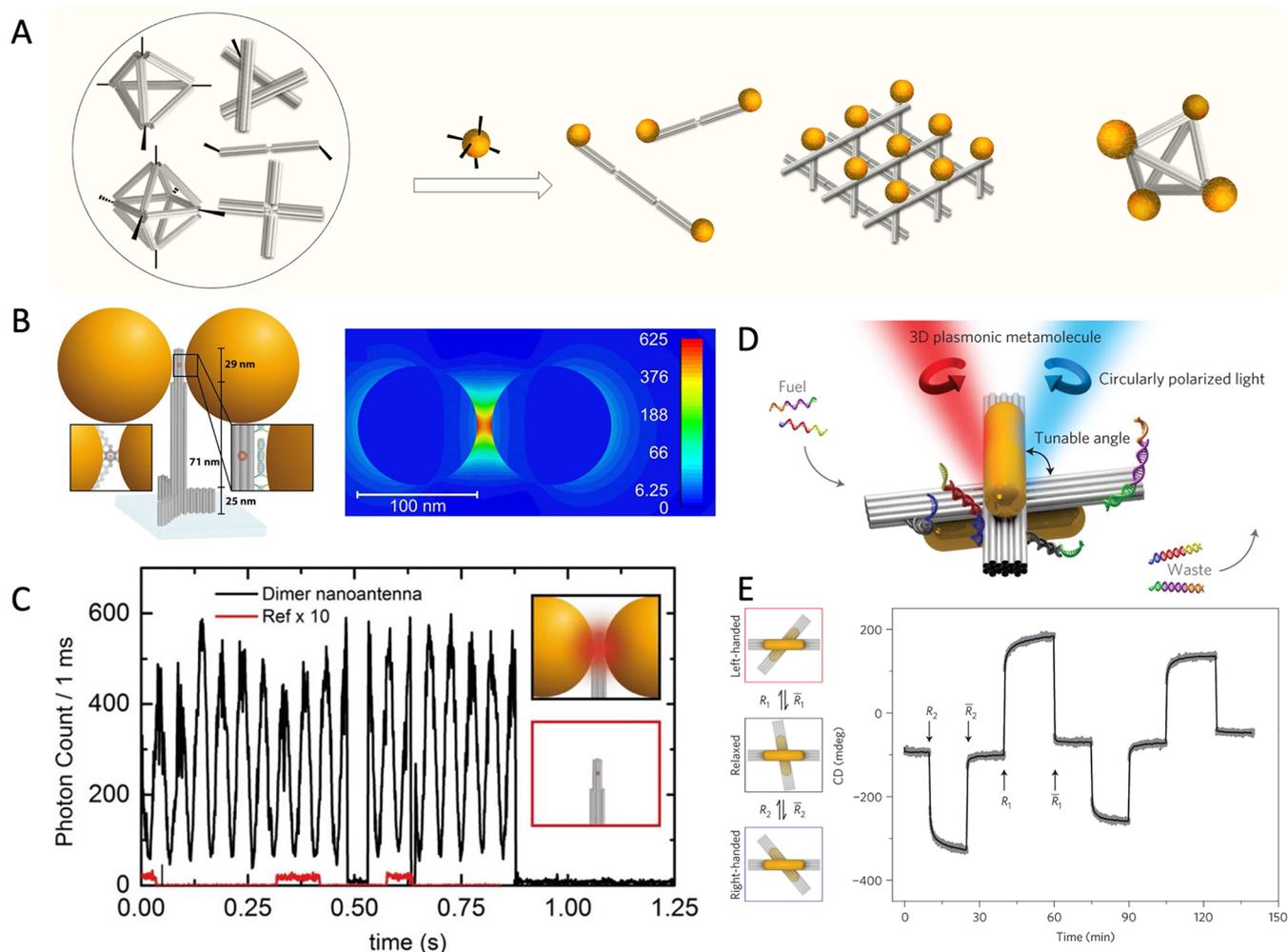


**Figure 3.** (A) Schematic illustration of the programmable directional assembly of NCs in a DNA template. (B) Sketch of the DNA origami and two Au NCs to assemble the optical nanoantenna (left), and its numerical simulation of the electric field intensity (right). (C) Single-molecule fluorescence transient response for the dimer nanoantenna (black line) or the DNA origami without NCs (red line) at ten times excitation intensity. Reproduced with permission from ref 98. Copyright (2015) American Chemical Society. (D) Schematic diagram of the tunable angle Au nanorods hosted on switchable DNA origami template. (E) The circularly polarized light of plasmonic nanostructure modulated by switchable DNA templates. Reproduced with permission from ref 94. Copyright (2014) Springer Nature.

a rational scheme for decorating NCs in arbitrary patterns or precisely fixing different NCs in the desired position. As a proof of concept, Alivisatos and colleagues constructed the pyramid assembly and chiral arrangement of NCs through the programming nucleic acids framework, demonstrating that the larger DNA nanostructures can be exploited as templates to integrate the monodisperse NCs into complex three-dimensional structures.<sup>60</sup> Then, several groups developed the DNA origami-based NC assembly,<sup>92–96</sup> which achieved great changes in properties at macro-scales through the precise and dynamic displacement of NCs.<sup>92–94</sup> Concurrently, a series of improved functions based on the precise assembly of NCs have been found. For instance, Tinnefeld et al. assembled Au NCs dimer at a precise space distance through cylindrical DNA origami.<sup>97</sup> The properties of dimers with various sizes have been systematically analyzed, which provides a simple solution for the investigation of the overlapping plasmonic fields in metal NC systems.<sup>97</sup> Furthermore, it is predicted that the electric field intensity factor increased by more than 500 for the 100 nm-Au NC dimer with a gap of 12 nm at a dimer-parallel incident electric field polarization with a wavelength of

640 nm, which effectively improved the signals of single-molecule fluorescence transients (Figure 3B,C).<sup>98</sup> Keyser et al. proposed the 40 nm<sup>2</sup> DNA origami platforms as templates to assemble 40 nm Au NCs into dimer formation with a gap of  $3.3 \pm 1$  nm. They observed a 7-fold enhancement in the coefficient for surface-enhanced Raman scattering (SERS).<sup>99</sup> Meanwhile, Ke et al. developed a new type of modular DNA origami laden with magnetic NCs, which exhibit enhanced magnetic resonance imaging (MRI) contrast through the dynamic assembly of magnetic NCs.<sup>100</sup>

Furthermore, for the geometric features tuning of high-order anisotropic nanoscale building blocks, Liedl et al. developed a method for using DNA origami to guide the conformational changes of NRs assembly in order to modulate chirality, color, and intensity of nanodevice.<sup>94</sup> By using strand displacement reactions (SDR), a switchable DNA origami with two bundles was used to perform dynamic spatial reconstruction driven by fuel DNA strands (Figure 3D), changing the relative angle of plasmonic Au NRs into desired states and causing strong circular dichroism (CD) changes (Figure 3E).<sup>94</sup> Ke et al. constructed a 3D reconfigurable nanostructure by positioning

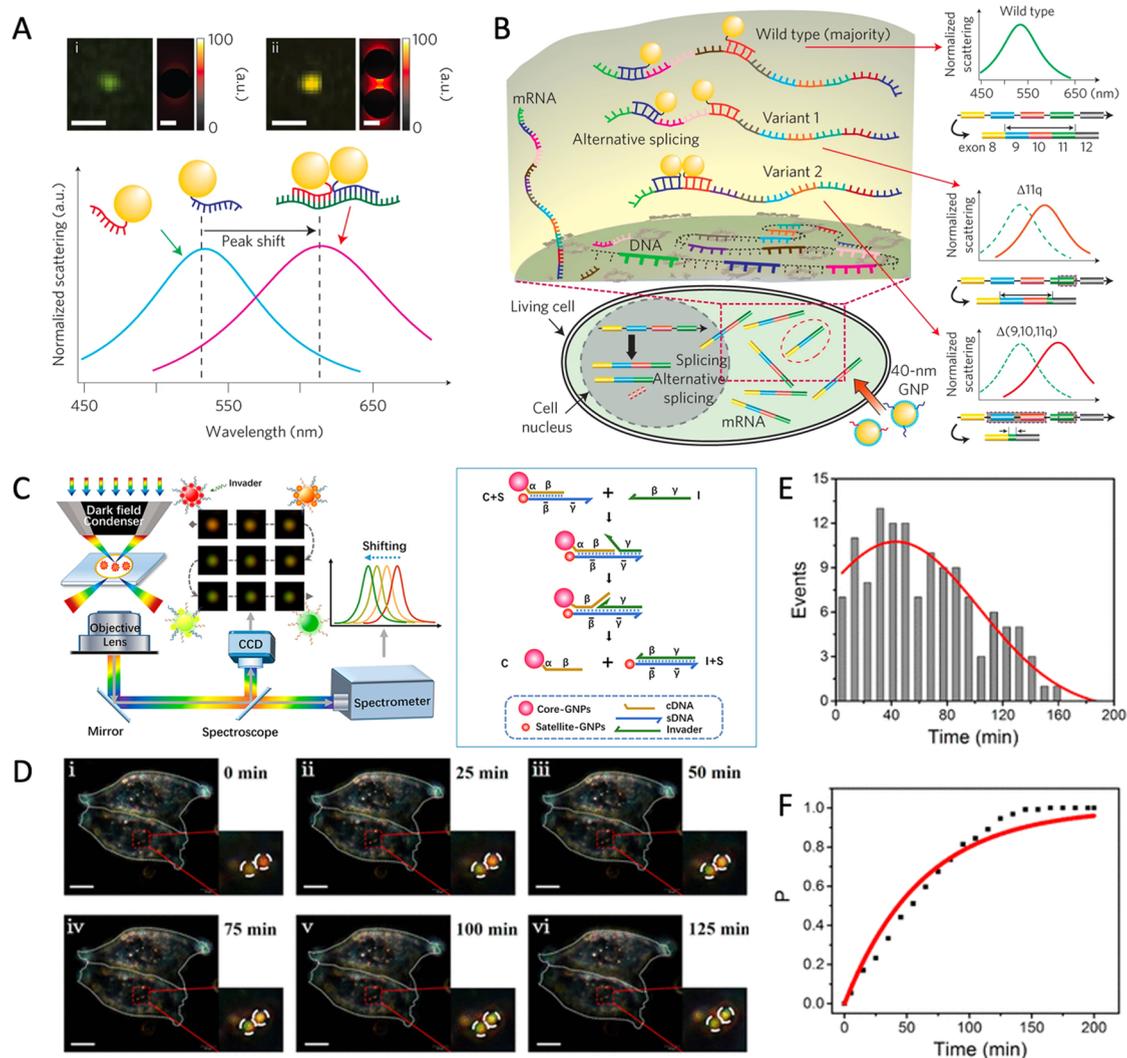


**Figure 4.** (A) Hyperspectral imaging and finite-difference time-domain simulation of monomeric and dimeric NCs. (B) The schematic diagram for single copy resolution imaging. Reproduced with permission from ref 119. Copyright (2014) Springer Nature. (C) Schematic illustration of the imaging model of core-satellite plasmon ruler (left) and the structure switching of plasmon ruler driven by toehold-mediated strand displacements (right). (D) The dark field microscope (DFM) imaging of plasmon ruler with time elapsing in living HeLa cells. Statistical analysis (E) of the disassembly events for the plasmon ruler, and cumulative probability (F) of the strand displacement in (D). Reproduced with permission from ref 120. Copyright (2018) American Chemical Society.

three Au NRs on a reconfigurable DNA tripod. The inter-nanorod distance and angle were precisely regulated through toehold-mediated strand displacement while operating the origami tripod.<sup>101</sup> Consequently, dynamic DNA origami nanotechnology has the potential to assemble high-order anisotropic building blocks, increase the complexity of coupling modes, and contribute to the development of signal conversion networks.<sup>94,102,103</sup>

### 3. DYNAMIC ASSEMBLY/DISASSEMBLY OF NCS FOR BIOMEDICAL IMAGING

Owing to the capability of structural conversion of DNA, well-designed DNA nanostructures allow for the dynamic assembly/disassembly of NCs, which can be applied in various biological stimulations<sup>104–106</sup> to enhance biomedical imaging.<sup>107,108</sup> This section focuses on DNA-driven dynamic assembly/disassembly of NCs with controllable optical and magnetic properties, and corresponding applications in biomedical imaging, in which the different interaction

approaches of manipulation such as Watson–Crick base pairing interactions, noncanonical base pairing interactions, aptamer–target interactions, and enzymatic/DNAzymatic reaction mediated covalent interactions are summarized.

#### 3.1. Watson–Crick Interaction

The Watson–Crick base-pairing interaction is crucial in both the control of nanoscaled DNA assembly and the regulation of dynamic DNA nanostructures. Most dynamic DNA systems are regulated by classical DNA-exchange reactions such as toehold-mediated SDR.<sup>109</sup> The toehold enables the displacement of the original strand by the binding strand, resulting in a change in DNA configuration and dynamic assembly/disassembly of DNA-NC conjugates. For example, Gang and coauthors reprogrammed the DNA-mediated interactions with the NCs, selectively manipulating the transformations between NC superlattices, which showed that DNA-exchange reactions enable dynamic reconfiguration and switchable structures in NC assembly,<sup>69</sup> providing multiple-stage activation and diverse functional capabilities.<sup>69,110,111</sup>

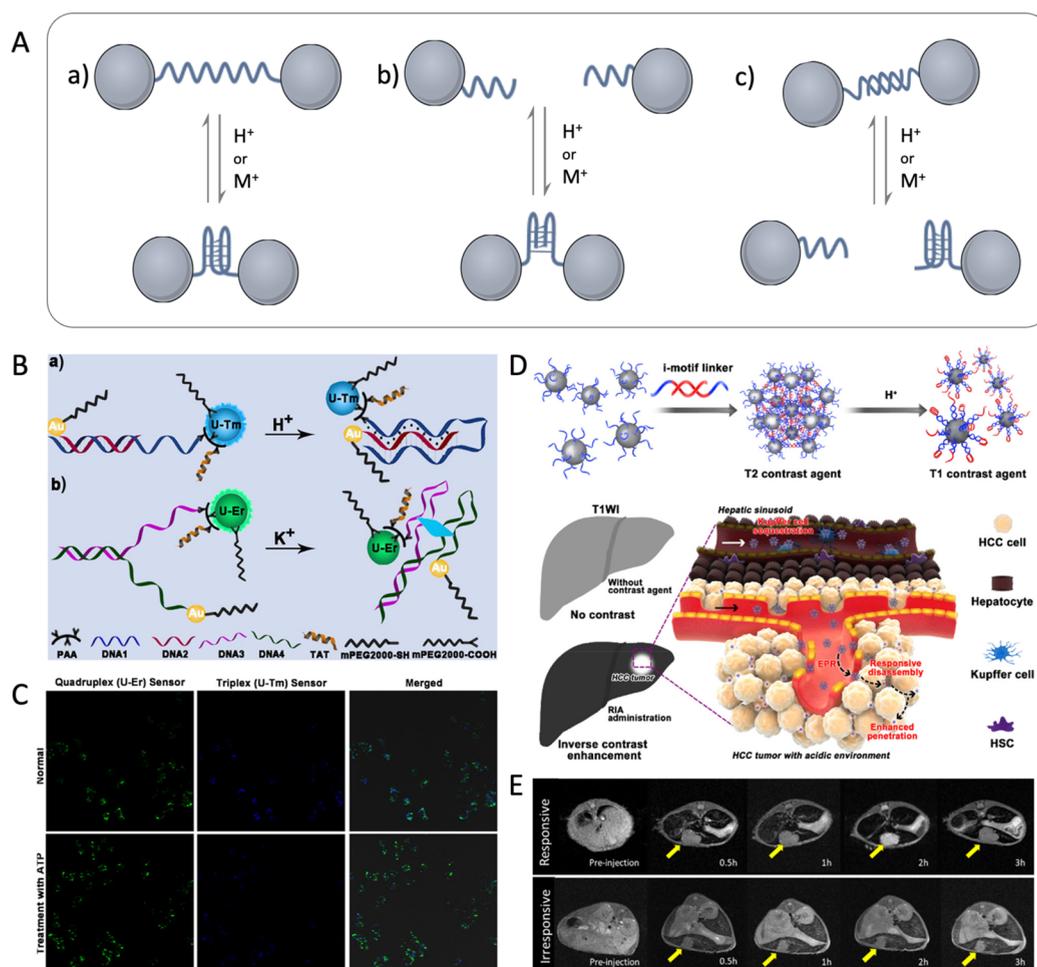


**Figure 5.** (A) Scheme for the general strategies for the design of NC assembly/disassembly driven by noncanonical DNA. (B) Schematic illustration of the principle of nanosensors based on (a) DNA triplex and (b) G-quadruplex for correlating pH and K<sup>+</sup> in lysosomes. (C) Confocal micrographs of HeLa cells with the signal change of nanosensors as stimulated by 100 μM ATP. Reproduced with permission from ref 129. Copyright (2021) Wiley-VCH GmbH, Weinheim. The (D) schematic diagram and (E) T1-weighted image of a pH MRI probe based on DNA i-motif applied for hepatocellular carcinoma imaging. Reproduced with permission from ref 130. Copyright (2018) American Chemical Society.

In the past decades, several new tools based on SDR have been developed for enhancing disease-related nucleic acid sensing, which demonstrates that DNA is capable of customizing dynamic NC assembly with controllable optical<sup>112</sup> and magnetic<sup>113</sup> properties, and expanding the applications of NCs in biomedical imaging.<sup>114,115</sup> For instance, Ma et al. created a quantum dots (QD) computing system based on fluorescence resonance energy transfer (FRET) through the dynamic assembly of polychromatic QD with DNA, which can image disease-related nucleic acid molecules (e.g., microRNA and mRNA).<sup>116</sup> Interacting with multiple nucleic acid targets, the imaging signals of QDs were generated, which improved the efficiency and accuracy of molecular diagnosis in vitro and in vivo.<sup>116</sup> In addition, the change in the assembly state of superparamagnetic NCs has sensitive and reversible impacts on the relaxation rate of adjacent water molecules. Weissleder's group developed a magnetic resonance (MR) switch for quantitative analysis of nucleic acids and identification of DNA sequences with single nucleotide mismatches.<sup>113,117</sup> These nanoswitches for MRI imaging are nontoxic to mammals without the limitation of penetration depth, providing a promising option for in vivo nucleic acid sequencing.<sup>117</sup> Moreover, Alivisatos et al. developed a DNA plasmonic ruler

to measure the distance between NCs, utilizing the DNA double helix as the linear template to control the NCs distance.<sup>85</sup> When plasmonic NCs approach one another, the scattering spectrum undergoes a spectral shift with the vibrant colors of NCs under a dark field microscope (DFM). This DNA plasmonic ruler offers a potential alternative to FRET for measuring nanoscale distances with a broader range and longer period, which is advantageous for sensing the interaction between biological macromolecules.<sup>85,118</sup> Irudayaraj et al. combined hyperspectral imaging with plasmon rulers made of dynamically assembling Au NCs in cells to detect single-molecule mRNA with precision (Figure 4A).<sup>119</sup> By measuring the position relationship of NCs which were captured by target sequence on mRNA, plasmon rulers monitored the spatial and temporal distribution of three selected splice variants of the breast cancer susceptibility gene BRCA1 in single copy resolution (Figure 4B).<sup>119</sup> Chen et al. fabricated a plasmon ruler composed of Au NCs core-satellite structures, which were controlled by the toehold-mediated strand displacement of complementary micro-RNA (Figure 4C).<sup>120</sup> The strand displacement induced by the target miRNA disassembles the plasmon ruler, resulting in synchronous changes in scattering intensity and wavelength in the DFM. Since miRNA gradually

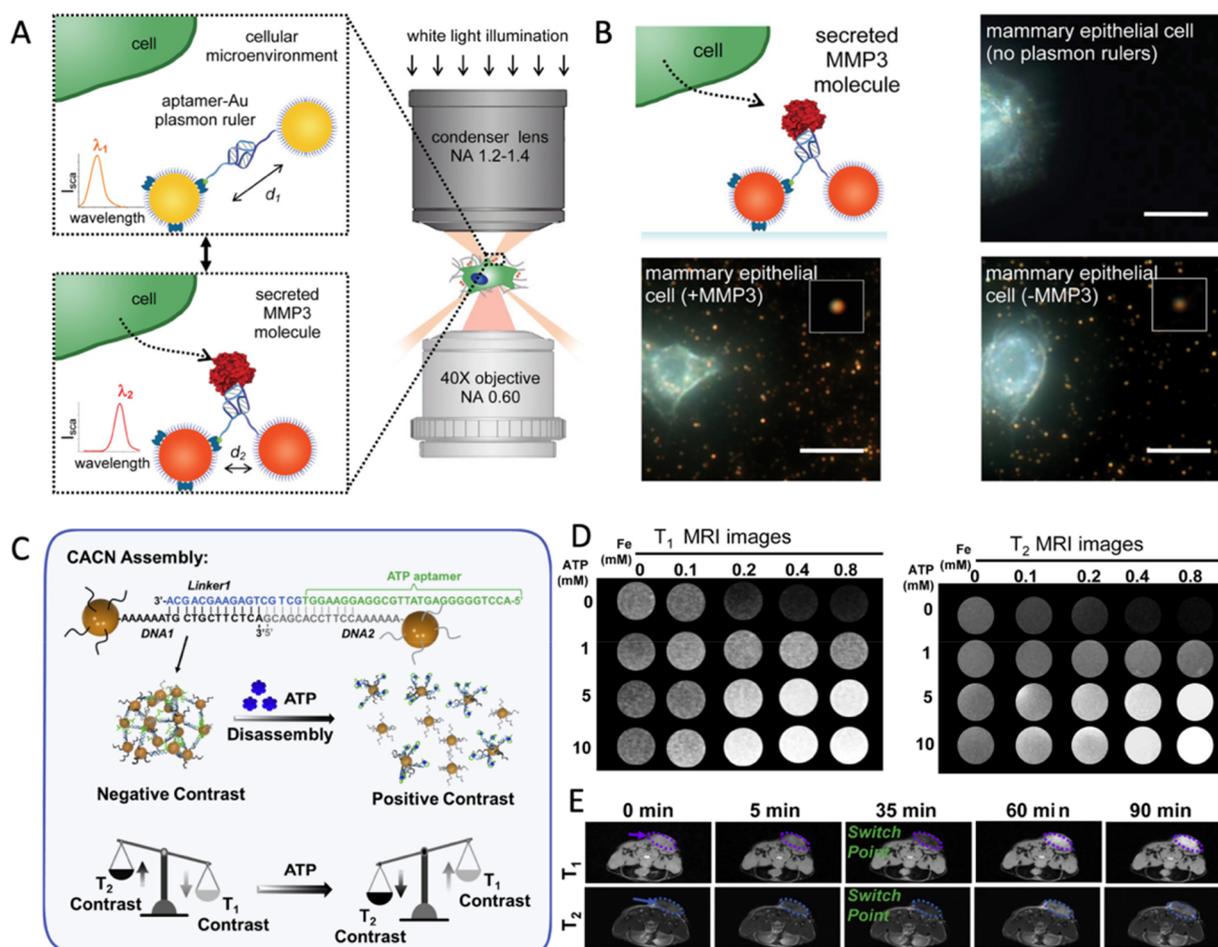


**Figure 6.** (A) The switchable distance strategy of aptamer-Au plasmon rulers, and (B) darkfield scattering images to measure secreted protein molecules in the cellular microenvironment. Reproduced with permission from ref 135. Copyright (2015) American Chemical Society. (C) Scheme for ATP-triggered disassembly of MRI probes with the T<sub>1</sub>/T<sub>2</sub> switchable. The T<sub>1</sub>-weighted and T<sub>2</sub>-weighted imaging of (D) in vitro and (E) in vivo triggered with various concentrations of ATP. Reproduced with permission from ref 142. Copyright (2022) Elsevier.

displaces, the color of the plasmon ruler changed from pink to yellow to green, allowing real-time detection of the dynamic biological distribution of miRNA 21 in HeLa cells at the single-molecule level (Figure 4D–F). The unique performance of plasmon rulers allows for single-molecule monitoring of biological processes in living cells.<sup>120</sup> DNA-driven dynamic NC assembly has great potential to overcome the limitations of conventional probes, such as photobleaching and photoblinking.<sup>85,118–120</sup> Furthermore, the described dynamic nano-assemblies are susceptible to “genetic” input, much like living matter is, potentially opening up new avenues for dynamic connections between biological and artificial systems. Undergoing the “genetic” modification to structural “evolution”, these dynamic inorganic nanocrystals have achieved a promising opportunity to mimic biological systems.<sup>69,70,101</sup>

### 3.2. Noncanonical Base-Pairing Interaction

Noncanonical base pairing occurs when bases interact differently from the standard Watson–Crick rules, which enriches the diversity of DNA structure and facilitates the development of functional modules.<sup>121,122</sup> Several DNA conformations function as natural gene regulators in specific pathological conditions, particularly the G-quadruplex<sup>121</sup> and the i-motif,<sup>122</sup> which form unique secondary structures through Hoogsteen base pairing or C:C<sup>+</sup> base pairing. For instance, the

low stability of G-quadruplex in K<sup>+</sup>-depleted environments is advantageous for gene transcription in invasive cancer cells containing the c-Myc protooncogene.<sup>123</sup> The formation of the secondary structures of i-motif requires weak acidic conditions, similar to the acidic tumor microenvironment.<sup>124,125</sup> Through conformation switching, the topological diversity and complexity of noncanonical DNA can provide a novel methodology for constructing nanoprobe.<sup>126</sup> As shown in Figure 5A, there are three general strategies for fabricating nanoprobe through noncanonical DNA secondary structures, which can form in specific disease microenvironments and drive the assembly or disassembly of NCs: (a) the formation of noncanonical conformation accompanied by multiple folds with the geometric change alters the distance between conjugated NCs;<sup>127</sup> (b) the assembly of NCs is driven by the intermolecular noncanonical conformation;<sup>127</sup> (c) DNA conformation switching between intramolecular noncanonical and double helix dynamically regulates the assembly/disassembly of NCs.<sup>128</sup>

At present, a series of probes based on noncanonical DNA-driven NC assembly have been developed. Liu et al. established a nanoprobe based on DNA triplets and G-quadruplex for the subcellular monitoring of K<sup>+</sup> and H<sup>+</sup> in the lysosomal cavity.<sup>129</sup> As the concentration of K<sup>+</sup> or H<sup>+</sup> increased, the DNA loading with UCNP and AuNP was

folded into triplets or quadruplexes, resulting in a shorter distance between UCNP and Au NC (Figure 5B), which can dynamically respond in the pH range of 5.0–8.2 and 5–200 mM of  $[K^+]$  conditions. Moreover, it is observed that the inflow of  $H^+$  is accompanied by the outflow of  $K^+$  during ATP-induced lysosomal acidification (Figure 5C).<sup>129</sup> In addition, for the early diagnosis of tumors, Ling et al. designed an intelligent MRI probe based on the i-motif DNA functionalized ultrasmall superparamagnetic iron oxide nanocrystals (USIONs).<sup>130</sup> The USIONs are assembled by the base pairing interaction of DNA, which can act as a responsive iron oxide nanocrystal assembly (RIA) with a high  $r_2/r_1$  ratio (63.28), resulting in normal liver darkening. Subsequently, the tumor acidic microenvironment induces the RIA disassembly with i-motif DNA conformation, then switches into monodisperse USIONs with ideal T1-weighted imaging performance ( $r_2/r_1 = 7.12$ ) (Figure 5D). Consequently, the normal tissues were darkened and the tumor tissues were brightened with a  $\sim 4$  times difference in signal intensity, which is highly valuable for the accurate imaging and early diagnosis of small hepatocellular carcinomas (Figure 5E).<sup>130</sup>

Besides the natural structures of G-quadruplex and i-motif, artificial noncanonical DNA structures have also been developed, such as metal base pairs<sup>131</sup> that have been applied in the detection of heavy metal ions and water quality.<sup>132</sup> While flexible base sequence programmability gives infinite possibilities to the DNA structures. We believe that more DNA interactions beyond the Watson–Crick rules could be discovered, which may further expand the applications of nanoprobe through the conformation switching of DNA structures.

### 3.3. Aptamer–Target Interaction

The DNA aptamer selected from the synthesis library has the ability to interact with certain bioactive molecules.<sup>133,134</sup> The strategies have been developed for biomedical imaging through changes in the assembly state of DNA-NC conjugates by altering the interaction between the DNA aptamer and bioactive molecules. The interconversion between secondary structure conformations formed by the interaction of DNA with target molecules and the DNA double helix can facilitate the assembly and disassembly of DNA-NC conjugates. This section focuses on the typical applications of biomedical imaging utilizing aptamer–target interaction-mediated DNA-NC conformation switching.

Bissell et al. developed reversible aptamer–Au plasmon rulers consisting of Au NCs coupled to a single aptamer strand.<sup>135</sup> When the aptamer interacts with a single protein molecule with a high level of specificity, the spatial changes in DNA structures can result in the distance regulation of NCs conjugation at both ends of DNA (Figure 6A). The combination of the target secretory molecule MMP3 with plasmon rulers shows a 12 nm red shift with single molecule sensitivity, allowing for the visualization and quantification of MMP3 molecules secreted in the microenvironment of mammary epithelial cells (Figure 6B).<sup>135</sup> The strategy showed great potential to characterize the spatiotemporal resolution of the secreted molecules' form and evolution in the cell microenvironment. Meanwhile, Tan's group created the first colorimetric technique for cancer cell imaging through the affinity between aptamer functionalized NCs and the target molecules.<sup>136</sup> The well-designed aptamer is capable of recognizing the target protein on the surface of cancer cell

membranes, and assembling the NCs to effectively enhance the interaction with light, allowing for the distinction of diverse types of cells based on the aptamer applied in the analysis. Then, they proved the universality of this targeted assembly methodology using a variety of NCs and aptamers to customize materials for fluorescent visualization of target cells.<sup>137–139</sup> Moreover, the competition between Watson–Crick interaction and aptamer–target interaction provides an additional assembly/disassembly strategy with precise controllability. For example, Lu et al. described a protocol for disassembling purple Au NC assembly into red Au NCs through aptamer–target interaction, in which the aptamer sequence is more likely to bind with analytes and block the base pair interaction sites.<sup>140</sup> Further utilized the interaction of ATP and related-aptamers as a model, they investigate the effect of the relative position of the non-base-pairing region between nucleotides and the Au NC surface.<sup>141</sup> Song et al. constructed an MRI probe based on the ultrasmall magnetic NC assembly, which can change contrast performance according to the ATP concentrations in tumor microenvironments and achieve better tumor resolution.<sup>142</sup> To enable ATP concentration-dependent disassembly, the probes were designed with a relative position between the pairing regions and the aptamers. As shown in Figure 6A, the linker 1-ATP aptamer strand connects DNA-NCs to act as ATP probes with the performance of T2 imaging in normal tissue. However, when probes detect an increase in ATP in the tumor microenvironment, the change in the aptamer conformation causes the probes to disassemble and switch the MRI from T2 to T1 contrast (Figure 6C), improving tumor resolution (Figure 6D,E).<sup>142</sup>

Moreover, owing to the technical advancements in the selection process and synthesis of aptamers, aptamer-based probes have favorable performance in advanced imaging technology, allowing for a wider range of biomarker analysis.<sup>143</sup> This shows that the aptamer-based dynamic NC assembly has the potential to broaden the scope of biomedical imaging to include more diverse bioactive molecules.

### 3.4. Enzymatic/DNAzymatic Reaction Mediated Covalent Interaction

Protein enzyme and DNAzyme reactions have extended the boundaries of programs operated by DNA-functionalized materials via manipulating chemical bonds.<sup>144</sup> Inspired by biological motors, the artificial DNA machines drive NCs to perform directional tasks via the conversion of chemical energy into controlled motions, which could be utilized as imaging probes for advanced imaging applications.<sup>145</sup>

A series of enzymes have been created in nature to regulate DNA replication, transmission, error correction, and other life processes in order to effectively manage genetic information.<sup>144,146</sup> It has been demonstrated that the DNA-related enzymes are equally active with DNA-NC conjugates,<sup>147–149</sup> indicating that the natural enzyme toolkits could be employed to create a more advanced dynamic assembly/disassembly process, even expand the replication and repair functions of DNA-NC assembly.<sup>146</sup> Kanaras et al. introduced the concept of protection and deprotection steps into NC assembly strategy using enzymes.<sup>147</sup> Restriction enzymes such as *EcoRI*, *StyI*, and others are used to cleave DNA duplexes on NCs at specific recognition sites to generate cohesive ends. Then, T4 DNA ligase is used to covalently link the nucleic acid backbone at the hybrid cohesive ends, increasing the diversity

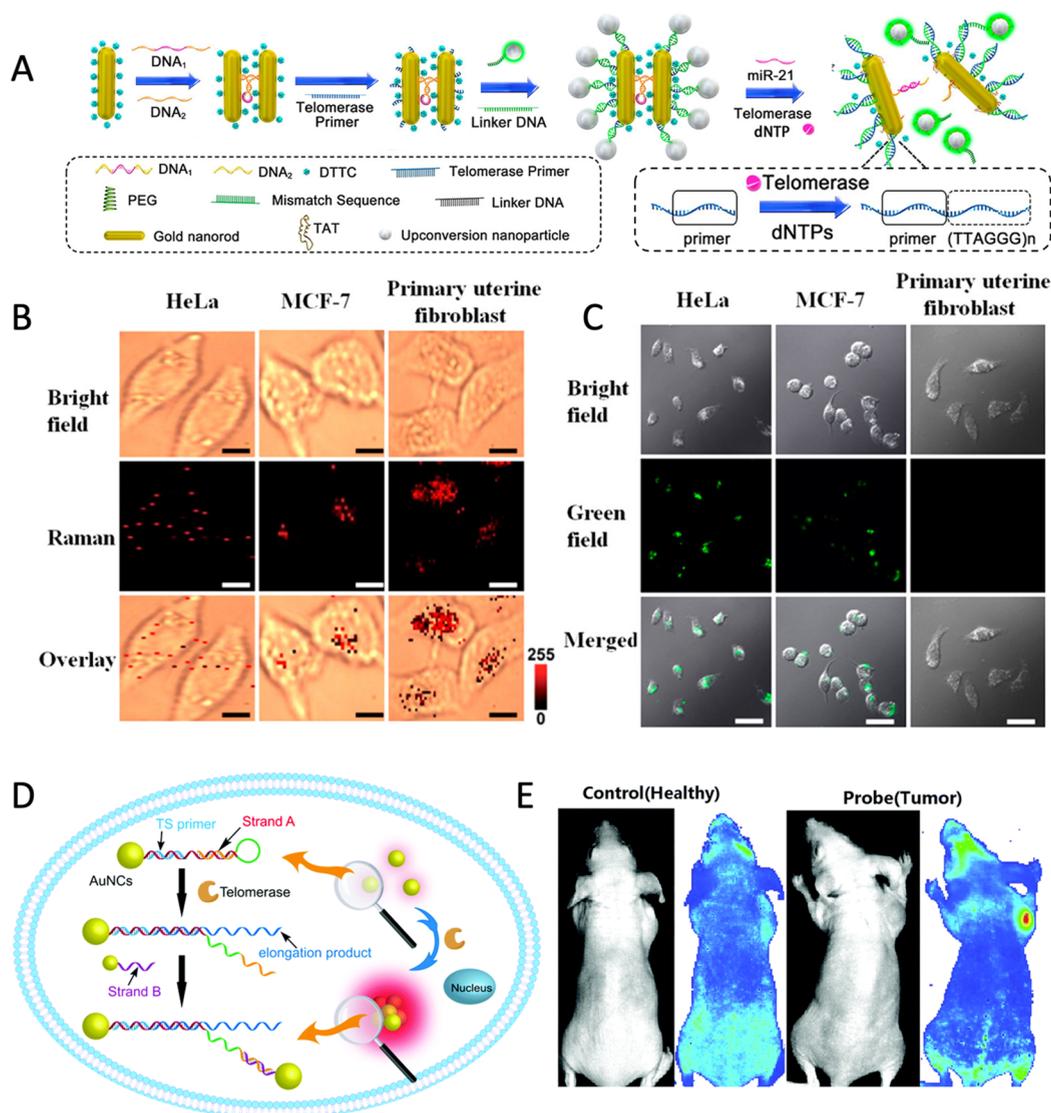


**Figure 7.** (A) Schematic illustration of the designed fabrication of the self-assembled satellite nanostructures of Au NR-dimer and UCNP and their bioresponsive disassembly process. (B) Raman imaging and (C) confocal images of HeLa, MCF-7, and primary uterine fibroblast cells with core-satellite assemblies. Reproduced with permission from ref 159. Copyright (2017) American Chemical Society. (D) Schematic illustration of the telomerase-triggered DNA hybridization/substitution that can drive NC assembly. (E) The telomerase fluorescence imaging in healthy mice and tumor mice. Reproduced with permission from ref 160. Copyright (2021) Royal Society of Chemistry.

of the assembly/disassembly of the DNA-NCs conjugation system.<sup>147,150</sup> The protection/deprotection approach of NC assembly, similar to protecting-group chemistry, allows NCs to be programmed and manipulated to synthesize nanoassembled structures by selectively blocking and activating their functionality.<sup>151</sup> The use of enzyme toolkits has increased the possibilities for dynamic assembly/disassembly of NCs, with the discovery of more than 3000 restrictive enzymes (hundreds of which are commercially available).<sup>147</sup> In addition, enzyme-assisted reactions improve the traditional DNA motor mode driven by SDR.<sup>152,153</sup> The free energy generated by the enzyme acting on DNA covalent bonds triggers the next step of SDR and drives DNA information transmission.<sup>144,154</sup> Based on this fact, it opens up the possibility of developing a novel DNA motor with autonomous, unidirectional, and progressive linear translational motion.<sup>144</sup> For instance, Salaita et al. developed a DNA rolling machine, which utilizes RNase H to selectively hydrolyze highly multivalent DNA-RNA duplexes

on spherical particles as the driving force, resulting in an increase in movement by 3 orders of magnitude compared with the traditional DNA walkers.<sup>145</sup> Wang et al. developed a 3D DNA rolling machine by integrating DNA walkers with Ag NCs to recognize the target and expose the toes for rolling, which provides the cascaded amplified signals.<sup>155</sup> With an efficient chemical/mechanical energy conversion efficiency to amplify the signal of biomarkers, a DNA rolling machine driven by enzymes has achieved the accurate detection of p53 gene in blood samples,<sup>155</sup> as well as the imaging of single nucleotide polymorphism (SNP) for simple equipment, allowing the possibility of imaging biomarkers with functional DNA such as aptamers. For in vivo imaging, the interactions between DNA and various enzymes can be designed to dynamically assemble NCs for the sensing of highly expressed enzymes in the disease microenvironment. Telomerase, which is highly expressed in most cancer cells, is essential for cancer diagnosis.<sup>156,157</sup> DNA ligands can be designed to monitor

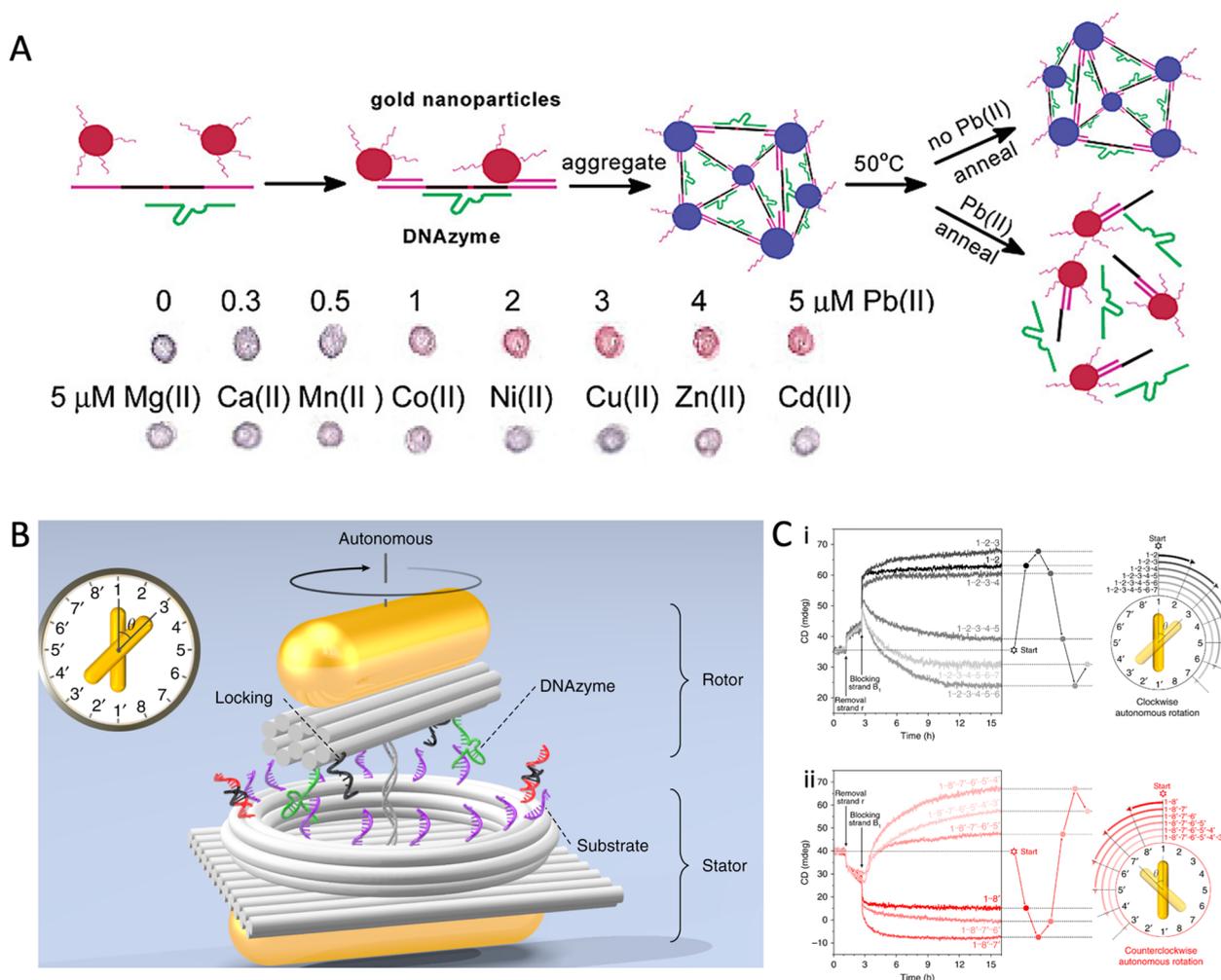


**Figure 8.** (A) Schematic illustration of DNAzyme-directed assembly of Au NCs and their sensing imaging with  $\text{Pb}^{2+}$  ions and interferent ions. Reproduced with permission from ref 167. Copyright (2003) American Chemical Society. (B) Schematic illustration of the rotary plasmonic nanoclock for autonomous rotation. (C) Time-course CD measurement for clockwise autonomous rotation (i) and counterclockwise autonomous rotation (ii). Reproduced with permission from ref 177. Copyright (2019) Springer Nature.

telomerase activity *in vivo* by driving the assembly and disassembly of NCs. Wang et al. reported Au<sub>50</sub>@Au<sub>13</sub> core-satellite nanostructures assembled by two sizes of Au NCs functionalized by DNA.<sup>158</sup> Telomerase extends a repeat sequence  $(\text{TTAGGG})_n$ , the telomerase primer (TP), and then releases the complementary strands to drive Au NC assembly, which realizes the significant blue shift of the LSPR spectrum and *in situ* monitoring of the change of telomerase activity.<sup>158</sup> Wei et al. used DNA programming to assemble Au NRs and UCNP, including two Au NRs (forming a dimer structure) as a core and the UCNP as satellites (Figure 7A).<sup>159</sup> Then, Micro-RNA 21 triggered the disassembly of the Au NR dimer and telomerase released the UCNP, generating two independent signals in living cells: a Raman signal from Au NR (Figure 7B) and a fluorescence signal from UCNP (Figure 7C).<sup>159</sup> Qu et al. designed a hairpin-shaped TP DNA modified on Au NC to respond to telomerase.<sup>160</sup> When internalized by cancer cells and recognized telomerase, the TP DNA could be extended and replaced to release a toehold domain of strand A, which subsequently interacted with strand B of another Au NC to generate the aggregation-induced emission (AIE) effect resulting from the assembly of Au NCs, allowing for the selective imaging of telomerase activity in living tumor cells *in*

*vitro* and *in vivo* (Figure 7D,E).<sup>160</sup> However, the limited number of enzymes with both disease markers and DNA conformation-switching properties restricts their application in biomedical imaging. Recently, chemical modification of DNA skeletons has been considered as a means of expanding the enzymatic toolkit to construct DNA nanoprobes for identifying highly expressed enzymes in diverse disease microenvironments. DNA probes containing molecular beacons at apurinic/pyrimidic sites, for instance, can identify the human apurinic/pyrimidic endonuclease 1 in the inflammatory microenvironment<sup>161</sup> or tumor microenvironment.<sup>162</sup> The capability of peptide-modified nucleic acid triblock copolymers to identify highly expressed proteases in the tumor microenvironment<sup>163</sup> demonstrates the potential of using DNA chemical engineering approaches to customize the nanoprobes driven by enzymes.

Additionally, since the discovery of catalytic nucleic acid (ribozyme), researchers have screened a series of DNAzymes with both programmability and catalytic activity, which is highly valuable for biosensor and medical diagnosis applications.<sup>164</sup> DNAzyme has excellent affinity and selectivity for a certain biological target, allowing for the controlled capture and release of target DNA.<sup>164</sup> Typically, the catalytic core of DNAzyme is maintained by the complexation of specific metal

ions, which catalyzes the formation or breaking of phosphate diester bonds with target DNA or RNA.<sup>165</sup> Therefore, DNAzyme is ideally suited for the construction of metal ion probes, which are capable of combining with ion specificity and catalyzing the substrate strand to drive the dynamic assembly of NCs.<sup>165,166</sup> For example, Lu et al. reported a Pb<sup>2+</sup> sensor based on a blue-colored aggregate composed of DNAzyme and AuNP-tagged substrate; in the presence of Pb<sup>2+</sup>, the DNAzyme cleaves the substrate strand, disassembling the AuNP aggregate and leading to a color change from blue to red (Figure 8A).<sup>167</sup> DNAzymes can identify metal ions and drive the dynamic assembly/disassembly of Au NCs for a visual color change,<sup>167,168</sup> which have acted as portable biosensors, such as transverse flow devices<sup>169,170</sup> and paper sensors.<sup>171,172</sup> In addition, driving magnetic NCs for dynamic assembly stimulated by metal ions, DNAzyme has also been proven to be useful for MRI detection.<sup>173,174</sup> Furthermore, due to DNA's physical and chemical properties, DNAzymes can be engineered to act as advanced molecular machines that can control the behavior of NCs to conduct complex mechanical tasks such as "walking", "splitting", and "rotating".<sup>175–177</sup> For instance, Choi and colleagues reported a DNA motor that can walk along the nanotube.<sup>176</sup> DNAzyme converts the chemical energy from the substrate RNA on the nanotube into movement, driving the CdS NCs along the orbit in a programmatic manner. The movement of a single NC was observed in real-time with dual visible/near-infrared optical spectroscopy.<sup>176</sup> Inspired by ATP synthetase, Liu et al. created a rotating plasma nanoclock made of DNA and Au NR.<sup>177</sup> Two Au NRs are assembled and immobilized into stator and rotor by DNA, respectively. The rotor is able to rotate in a reversible, and omnidirectional manner, driven by DNAzyme-RNA interactions, which can be monitored in real-time using optical spectroscopy (Figure 8B).<sup>177</sup> By leveraging the high energy conversion efficiency of DNAzyme and the exquisite programmability of DNA, it is anticipated that DNAzyme toolkits can enhance the capabilities of DNA and accelerate the speed of NC movement in programs with delicate signals of biological markers, making huge progress in the field of biomedical imaging.

Overall, switching DNA configurations, through natural biological processes or synthetic chemical modifications, has broadened the scope of using dynamic assembly/disassembly of NCs for the specific imaging of various biomarkers. Furthermore, with the use of editable DNA, it is easy to alter the sequence of an interaction region to specifically respond to target molecules, creating a useful toolbox for developing universal and modular platforms for advanced biomedical imaging and clinical diagnoses.

#### 4. CONCLUSION

The controllable assembly/disassembly of inorganic NCs remains a major challenge in nanotechnology. DNA nanotechnology provides a promising method tool to arrange NCs precisely into assemblies with the desired optical, electrical, or magnetic properties.<sup>93</sup> Although several biomedical imaging strategies have been proposed based on DNA-driven dynamic assembly of NCs, the relevant research remains in its infancy, and there are still several challenges to be addressed. First, in order to enrich the library of structures for NC self-assembly, reasonable surface engineering is urgently needed to improve the modification efficiency of DNA with NCs, which enables more precise and programmable assembly with inorganic NCs,

especially those without DNA affinity on surface sites. Second, DNA not only can manipulate the assembly state of NCs, but also has the potential to directly affect imaging-related parameters owing to their unique structures. For instance, when close to guanine-rich DNA sequences, the red fluorescence of DNA/Ag NCs is greatly amplified.<sup>178</sup> The extensive and in-depth studies on the mechanisms of DNA that promote the imaging performance of NCs are helpful in expanding the applications of DNA-driven NC assembly in biomedical imaging. Third, the DNA-based dynamic NC assembly in response to a single endogenous stimulus (e.g., pH, redox, enzyme) could suffer from nonspecific excitation by the nontarget area in the complex microenvironments in vivo, resulting in false-positive imaging results. Notably, the design of DNA-driven NC assembly with responsiveness on both endogenous and exogenous stimuli (e.g., light, sound, magnetic) holds promise to improve the response accuracy and imaging specificity through precise spatial–temporal manipulation.

Taken together, DNA nanotechnology has revolutionized inorganic NC assembly with precise and programmable features, leading to the creation of functional materials with customized chemical and physical properties. Then, by utilizing stimuli-responsive DNA, dynamic NC assembly has been produced with the potential for sensing various biomarkers. Through "genetic" modification, NCs could undergo structural "evolution", providing a methodology for the designed fabrication of advanced biomedical probes with outstanding imaging performance.

#### AUTHOR INFORMATION

##### Corresponding Authors

**Fangyuan Li** – Institute of Pharmaceutics, College of Pharmaceutical Sciences, Zhejiang University, Hangzhou 310058, P. R. China; World Laureates Association (WLA) Laboratories, Shanghai 201203, P. R. China; Hangzhou Institute of Innovative Medicine, Zhejiang University, Hangzhou 310058, P. R. China; [orcid.org/0000-0002-8086-7362](https://orcid.org/0000-0002-8086-7362); Email: [lfy@zju.edu.cn](mailto:lfy@zju.edu.cn)

**Daishun Ling** – Frontiers Science Center for Transformative Molecules, School of Chemistry and Chemical Engineering, National Center for Translational Medicine, State Key Laboratory of Oncogenes and Related Genes, Shanghai Jiao Tong University, Shanghai 200240, P. R. China; World Laureates Association (WLA) Laboratories, Shanghai 201203, P. R. China; Hangzhou Institute of Innovative Medicine, Zhejiang University, Hangzhou 310058, P. R. China; [orcid.org/0000-0002-9977-0237](https://orcid.org/0000-0002-9977-0237); Email: [dsling@sjtu.edu.cn](mailto:dsling@sjtu.edu.cn)

##### Authors

**Shengfei Yang** – Institute of Pharmaceutics, College of Pharmaceutical Sciences, Zhejiang University, Hangzhou 310058, P. R. China

**Yuqi Wang** – Frontiers Science Center for Transformative Molecules, School of Chemistry and Chemical Engineering, National Center for Translational Medicine, State Key Laboratory of Oncogenes and Related Genes, Shanghai Jiao Tong University, Shanghai 200240, P. R. China; World Laureates Association (WLA) Laboratories, Shanghai 201203, P. R. China

**Qiyue Wang** – Frontiers Science Center for Transformative Molecules, School of Chemistry and Chemical Engineering,

National Center for Translational Medicine, State Key Laboratory of Oncogenes and Related Genes, Shanghai Jiao Tong University, Shanghai 200240, P. R. China; World Laureates Association (WLA) Laboratories, Shanghai 201203, P. R. China

Complete contact information is available at:  
<https://pubs.acs.org/10.1021/cbmi.3c00028>

### Author Contributions

#S. Yang, Y. Wang, and Q. Wang contributed equally.

### Notes

The authors declare no competing financial interest.

### ACKNOWLEDGMENTS

The authors acknowledge financial support by the National Key Research and Development Program of China (2022YFB3203801, 2022YFB3203804, 2022YFB3203800), the Leading Talent of “Ten Thousand Plan”-National High-Level Talents Special Support Plan, National Natural Science Foundation of China (32071374), Program of Shanghai Academic Research Leader under the Science and Technology Innovation Action Plan (21XD1422100), Program of Shanghai Science and Technology Development (22TS1400700), Zhejiang Provincial Natural Science Foundation of China (LR22C100001), Innovative Research Team of High-Level Local Universities in Shanghai (SHSMU-ZDCX20210900), and CAS Interdisciplinary Innovation Team (JCTD-2020-08).

### VOCABULARY

NC, inorganic nanocrystals: Inorganic nanocrystals are special particles that are composed of atoms in either a single- or poly-crystalline arrangement, with sizes typically in the range of 1–100 nm; PAEs, programmable atom equivalents: Programmable atom equivalents are oligonucleotide–nanoparticle conjugates that emulate the behavior of individual atoms, allowing for the precise assembly of larger structures; SERS, surface-enhanced Raman scattering: Surface-enhanced Raman scattering is a spectroscopic technique that enhances the Raman scattering signal of molecules adsorbed on some nanostructures, leading to highly sensitive detection and analysis of trace amounts of molecules; MRI, magnetic resonance imaging: Magnetic resonance imaging is a non-invasive medical imaging technique that creates two and three-dimensional detailed anatomical images of living subjects; SDR, strand displacement reactions: Strand displacement reactions are biochemical processes in which a single-stranded nucleic acid molecule displaces a complementary strand from a double-stranded nucleic acid molecule.

### REFERENCES

- (1) Santos, P. J.; Gabrys, P. A.; Zornberg, L. Z.; Lee, M. S.; Macfarlane, R. J. Macroscopic materials assembled from nanoparticle superlattices. *Nature* **2021**, *591* (7851), 586–591.
- (2) Udayabhaskararao, T.; Altantzis, T.; Houben, L.; Coronado-Puchau, M.; Langer, J.; Popovitz-Biro, R.; Liz-Marzan, L. M.; Vukovic, L.; Kral, P.; Bals, S.; Klajn, R. Tunable porous nanoallotropes prepared by post-assembly etching of binary nanoparticle superlattices. *Science* **2017**, *358*, 514–518.
- (3) Wang, T.; Zhuang, J.; Lynch, J.; Chen, O.; Wang, Z.; Wang, X.; LaMontagne, D.; Wu, H.; Wang, Z.; CAO, Y. C. Self-assembled colloidal superparticles from nanorods. *Science* **2012**, *338* (6105), 358–363.

- (4) Li, N.; Wu, F.; Han, Z.; Wang, X.; Liu, Y.; Yi, C.; Ye, S.; Lu, G.; Yu, L.; Nie, Z.; Ding, B. Shape complementarity modulated self-assembly of nanoring and nanosphere hetero nanostructures. *J. Am. Chem. Soc.* **2020**, *142* (27), 11680–11684.
- (5) Jeong, H.; Park, W.; Kim, D. H.; Na, K. Dynamic nanoassemblies of nanomaterials for cancer photomedicine. *Adv. Drug Delivery Rev.* **2021**, *177*, 113954.
- (6) Ibanez, M.; Luo, Z.; Genc, A.; Piveteau, L.; Ortega, S.; Cadavid, D.; Dobrozhan, O.; Liu, Y.; Nachtegaal, M.; Zebarjadi, M.; Arbiol, J.; Kovalenko, M. V.; Cabot, A. High-performance thermoelectric nanocomposites from nanocrystal building blocks. *Nat. Commun.* **2016**, *7*, 10766.
- (7) Cheng, X.; Sun, R.; Yin, L.; Chai, Z.; Shi, H.; Gao, M. Light-Triggered Assembly of Gold Nanoparticles for photothermal therapy and photoacoustic imaging of tumors in vivo. *Adv. Mater.* **2017**, *29* (6), 1604894.
- (8) Lee, H.; Sun, E.; Ham, D.; Weissleder, R. Chip-NMR biosensor for detection and molecular analysis of cells. *Nat. Med.* **2008**, *14* (8), 869–874.
- (9) Li, F.; Liang, Z.; Liu, J.; Sun, J.; Hu, X.; Zhao, M.; Liu, J.; Bai, R.; Kim, D.; Sun, X.; Hyeon, T.; Ling, D. Dynamically reversible iron oxide nanoparticle assemblies for targeted amplification of T1-weighted magnetic resonance imaging of tumors. *Nano Lett.* **2019**, *19* (7), 4213–4220.
- (10) Park, W.; Na, K. Advances in the synthesis and application of nanoparticles for drug delivery. *Wiley Interdiscip. Rev. Nanomed. Nanobiotechnol.* **2015**, *7* (4), 494–508.
- (11) Begley, M. R.; Gianola, D. S.; Ray, T. R. Bridging functional nanocomposites to robust macroscale devices. *Science* **2019**, *364* (6447), eaav4299.
- (12) Boles, M. A.; Engel, M.; Talapin, D. V. Self-assembly of colloidal nanocrystals: from intricate structures to functional materials. *Chem. Rev.* **2016**, *116* (18), 11220–11289.
- (13) Oh, E.; Hong, M.-Y.; Lee, D.; Nam, S.-H.; Yoon, H. C.; Kim, H.-S. Inhibition Assay of biomolecules based on fluorescence resonance energy transfer (FRET) between quantum dots and gold nanoparticles. *J. Am. Chem. Soc.* **2005**, *127*, 3270–3271.
- (14) Maier, S. A.; Kik, P. G.; Atwater, H. A.; Meltzer, S.; Harel, E.; Koel, B. E.; Requicha, A. A. Local detection of electromagnetic energy transport below the diffraction limit in metal nanoparticle plasmon waveguides. *Nat. Mater.* **2003**, *2* (4), 229–232.
- (15) Lee, J.; Govorov, A. O.; Kotov, N. A. Nanoparticle assemblies with molecular springs: a nanoscale thermometer. *Angew. Chem., Int. Ed. Engl.* **2005**, *44* (45), 7439–7442.
- (16) Köker, T.; Tang, N.; Tian, C.; Zhang, W.; Wang, X.; Martel, R.; Pinaud, F. Cellular imaging by targeted assembly of hot-spot SERS and photoacoustic nanoprobe using split-fluorescent protein scaffolds. *Nat. Commun.* **2018**, *9*, 607.
- (17) Lee, J.; Hernandez, P.; Lee, J.; Govorov, A. O.; Kotov, N. A. Exciton-plasmon interactions in molecular spring assemblies of nanowires and wavelength-based protein detection. *Nat. Mater.* **2007**, *6* (4), 291–295.
- (18) Roller, E. M.; Besteiro, L. V.; Pupp, C.; Khorashad, L. K.; Govorov, A. O.; Liedl, T. Hot spot-mediated non-dissipative and ultrafast plasmon passage. *Nat. Phys.* **2017**, *13* (8), 761–765.
- (19) Patra, P. P.; Chikkaraddy, R.; Tripathi, R. P.; Dasgupta, A.; Kumar, G. V. Plasmofluidic single-molecule surface-enhanced Raman scattering from dynamic assembly of plasmonic nanoparticles. *Nat. Commun.* **2014**, *5*, 4357.
- (20) Halas, N. J.; Lal, S.; Chang, W.-S.; Link, S.; Nordlander, P. Plasmons in strongly coupled metallic nanostructures. *Chem. Rev.* **2011**, *111* (6), 3913–3961.
- (21) Ghosh, S. K.; Pal, T. Interparticle coupling effect on the surface plasmon resonance of gold nanoparticles: From Theory to Applications. *Chem. Rev.* **2007**, *107*, 4797–4862.
- (22) Prodan, E.; Radloff, C.; Halas, N. J.; Nordlander, P. A Hybridization Model for the Plasmon response of complex nanostructures. *Science* **2003**, *302* (5644), 419–422.

- (23) Nie, Z.; Petukhova, A.; Kumacheva, E. Properties and emerging applications of self-assembled structures made from inorganic nanoparticles. *Nat. Nanotechnol.* **2010**, *5* (1), 15–25.
- (24) Du, H.; Wang, Q.; Liang, Z.; Li, Q.; Li, F.; Ling, D. Designed fabrication of magnetic nanoprobes for ultra-high-field magnetic resonance imaging. *Nanoscale* **2022**, *14* (47), 17483–17499.
- (25) Aubret, A.; Martinet, Q.; Palacci, J. Metamachines of pluripotent colloids. *Nat. Commun.* **2021**, *12* (1), 6398.
- (26) Li, F.; Du, Y.; Liu, J.; Sun, H.; Wang, J.; Li, R.; Kim, D.; Hyeon, T.; Ling, D. Responsive assembly of upconversion nanoparticles for pH-activated and near-infrared-triggered photodynamic therapy of deep tumors. *Adv. Mater.* **2018**, *30* (35), 1802808.
- (27) Ling, D. Dynamic nanoassembly-based drug delivery systems on the horizon. *J. Controlled Release* **2021**, *339*, 547–552.
- (28) Peng, L.; Peng, H.; Liu, Y.; Wang, X.; Hung, C. T.; Zhao, Z.; Chen, G.; Li, W.; Mai, L.; Zhao, D. Spiral self-assembly of lamellar micelles into multi-shelled hollow nanospheres with unique chiral architecture. *Sci. Adv.* **2021**, *7*, eabi7403.
- (29) Jones, M. R.; Seeman, N. C.; Mirkin, C. A. Nanomaterials. Programmable materials and the nature of the DNA bond. *Science* **2015**, *347* (6224), 1260901.
- (30) Andersen, E. S.; Dong, M.; Nielsen, M. M.; Jahn, K.; Subramani, R.; Mamdouh, W.; Golas, M. M.; Sander, B.; Stark, H.; Oliveira, C. L.; Pedersen, J. S.; Birkedal, V.; Besenbacher, F.; Gothelf, K. V.; Kjems, J. Self-assembly of a nanoscale DNA box with a controllable lid. *Nature* **2009**, *459* (7243), 73–76.
- (31) Pinheiro, A. V.; Han, D.; Shih, W. M.; Yan, H. Challenges and opportunities for structural DNA nanotechnology. *Nat. Nanotechnol.* **2011**, *6* (12), 763–772.
- (32) Rothemund, P. W. Folding DNA to create nanoscale shapes and patterns. *Nature* **2006**, *440* (7082), 297–302.
- (33) Gerling, T.; Wagenbauer, K. F.; Neuner, A. M.; Dietz, H. Dynamic DNA devices and assemblies formed by shape-complementary, non–base pairing 3D components. *Science* **2015**, *347* (6229), 1446–1452.
- (34) Benson, E.; Mohammed, A.; Gardell, J.; Masich, S.; Czeizler, E.; Orponen, P.; Hogberg, B. DNA rendering of polyhedral meshes at the nanoscale. *Nature* **2015**, *523* (7561), 441–444.
- (35) Majewski, P. W.; Michelson, A.; Cordeiro, L.; Tian, C.; Ma, C.; Kisslinger, K.; Tian, Y.; Liu, W.; Stach, E. A.; Yager, K. G.; Gang, O. Resilient three-dimensional ordered architectures assembled from nanoparticles by DNA. *Sci. Adv.* **2021**, *7* (12), No. eabf0617.
- (36) Ma, W.; Zhan, Y.; Zhang, Y.; Mao, C.; Xie, X.; Lin, Y. The biological applications of DNA nanomaterials: current challenges and future directions. *Signal Transduct. Target. Ther.* **2021**, *6* (1), 351.
- (37) Dong, Y.; Yao, C.; Zhu, Y.; Yang, L.; Luo, D.; Yang, D. DNA functional materials assembled from branched DNA: design, synthesis, and applications. *Chem. Rev.* **2020**, *120* (17), 9420–9481.
- (38) Zhang, Y.; Lu, F.; Yager, K. G.; van der Lelie, D.; Gang, O. A general strategy for the DNA-mediated self-assembly of functional nanoparticles into heterogeneous systems. *Nat. Nanotechnol.* **2013**, *8* (11), 865–872.
- (39) Auyeung, E.; Li, T. I.; Senesi, A. J.; Schmucker, A. L.; Pals, B. C.; de la Cruz, M. O.; Mirkin, C. A. DNA-mediated nanoparticle crystallization into Wulff polyhedra. *Nature* **2014**, *505* (7481), 73–77.
- (40) Macfarlane, R. J.; Lee, B.; Jones, M. R.; Harris, N.; Schatz, G. C.; Mirkin, C. A. Nanoparticle superlattice engineering with DNA. *Science* **2011**, *334* (6053), 204–208.
- (41) Lin, Q.-Y.; Mason, J. A.; Li, Z.; Zhou, W.; O'Brien, M. N.; Brown, K. A.; Jones, M. R.; Butun, S.; Lee, B.; Dravid, V. P.; Aydin, K.; Mirkin, C. A. Building superlattices from individual nanoparticles via template-confined DNA-mediated assembly. *Science* **2018**, *359* (6376), 669–672.
- (42) Kim, Y.; Macfarlane, R. J.; Jones, M. R.; Mirkin, C. A. Transmutable nanoparticles with reconfigurable surface ligands. *Science* **2016**, *351* (6273), 579–582.
- (43) Ross, M. B.; Ku, J. C.; Blaber, M. G.; Mirkin, C. A.; Schatz, G. C. Defect tolerance and the effect of structural inhomogeneity in plasmonic DNA-nanoparticle superlattices. *Proc. Natl. Acad. Sci. U.S.A.* **2015**, *112* (33), 10292–10297.
- (44) Wang, Y.; Nguyen, K.; Spitale, R. C.; Chaput, J. C. A biologically stable DNzyme that efficiently silences gene expression in cells. *Nat. Chem.* **2021**, *13* (4), 319–326.
- (45) Thompson, I. A. P.; Zheng, L.; Eisenstein, M.; Soh, H. T. Rational design of aptamer switches with programmable pH response. *Nat. Commun.* **2020**, *11* (1), 2946.
- (46) Zhang, Q. L.; Wang, L. L.; Liu, Y.; Lin, J.; Xu, L. A kinetically controlled platform for ligand-oligonucleotide transduction. *Nat. Commun.* **2021**, *12* (1), 4654.
- (47) Wu, L.; Wang, Y.; Xu, X.; Liu, Y.; Lin, B.; Zhang, M.; Zhang, J.; Wan, S.; Yang, C.; Tan, W. Aptamer-based detection of circulating targets for precision medicine. *Chem. Rev.* **2021**, *121* (19), 12035–12105.
- (48) Zhao, S.; Tian, R.; Wu, J.; Liu, S.; Wang, Y.; Wen, M.; Shang, Y.; Liu, Q.; Li, Y.; Guo, Y.; Wang, Z.; Wang, T.; Zhao, Y.; Zhao, H.; Cao, H.; Su, Y.; Sun, J.; Jiang, Q.; Ding, B. A DNA origami-based aptamer nanoarray for potent and reversible anticoagulation in hemodialysis. *Nat. Commun.* **2021**, *12* (1), 358.
- (49) Zhao, Y.; Shi, L.; Kuang, H.; Xu, C. DNA-driven nanoparticle assemblies for biosensing and bioimaging. *Top. Curr. Chem.* **2020**, *378* (1), 18.
- (50) Samanta, A.; Medintz, I. L. Nanoparticles and DNA - a powerful and growing functional combination in bionanotechnology. *Nanoscales* **2016**, *8* (17), 9037–9095.
- (51) Li, L.; Xing, H.; Zhang, J.; Lu, Y. Functional DNA molecules enable selective and stimuli-responsive nanoparticles for biomedical applications. *Acc. Chem. Res.* **2019**, *52* (9), 2415–2426.
- (52) He, L.; Mu, J.; Gang, O.; Chen, X. Rationally programming nanomaterials with dna for biomedical applications. *Adv. Sci.* **2021**, *8* (8), 2003775.
- (53) Bathe, M.; Rothemund, P. W. K. DNA nanotechnology: a foundation for programmable nanoscale materials. *MRS Bull.* **2017**, *42* (12), 882–888.
- (54) Seeman, N. C.; Sleiman, H. F. DNA nanotechnology. *Nat. Rev. Mater.* **2018**, *3* (1), 17068.
- (55) Zhang, F.; Jiang, S.; Wu, S.; Li, Y.; Mao, C.; Liu, Y.; Yan, H. Complex wireframe DNA origami nanostructures with multi-arm junction vertices. *Nat. Nanotechnol.* **2015**, *10* (9), 779–784.
- (56) Mirkin, C. A.; Letsinger, R. L.; Mucic, C.; Storhoff, J. J. A DNA-based method for rationally assembling nanoparticles into macroscopic materials. *Nature* **1996**, *382*, 607–609.
- (57) Alivisatos, A. P.; Johnsson, K. P.; Peng, X.; Wilson, T. E.; Loweth, C. J.; Bruchez, M. P., Jr; Schultz, P. G. Organization of 'nanocrystal molecules' using DNA. *Nature* **1996**, *382* (15), 609–611.
- (58) De Fazio, A. F.; Misatziou, D.; Baker, Y. R.; Muskens, O. L.; Brown, T.; Kanaras, A. G. Chemically modified nucleic acids and DNA intercalators as tools for nanoparticle assembly. *Chem. Soc. Rev.* **2021**, *50* (23), 13410–13440.
- (59) Julin, S.; Nummelin, S.; Kostianen, M. A.; Linko, V. DNA nanostructure-directed assembly of metal nanoparticle superlattices. *J. Nanopart. Res.* **2018**, *20* (5), 119.
- (60) Mastroianni, A. J.; Claridge, S. A.; Alivisatos, A. P. Pyramidal and chiral groupings of gold nanocrystals assembled using DNA scaffolds. *J. Am. Chem. Soc.* **2009**, *131* (24), 8455–8459.
- (61) Macfarlane, R. J.; O'Brien, M. N.; Petrosko, S. H.; Mirkin, C. A. Nucleic acid-modified nanostructures as programmable atom equivalents: forging a new "table of elements". *Angew. Chem., Int. Ed. Engl.* **2013**, *52* (22), 5688–5698.
- (62) Nykypanchuk, D.; Maye, M. M.; van der Lelie, D.; Gang, O. DNA-guided crystallization of colloidal nanoparticles. *Nature* **2008**, *451* (7178), 549–552.
- (63) Park, S. Y.; Lytton-Jean, A. K.; Lee, B.; Weigand, S.; Schatz, G. C.; Mirkin, C. A. DNA-programmable nanoparticle crystallization. *Nature* **2008**, *451* (7178), 553–556.
- (64) Senesi, A. J.; Eichelsdoerfer, D. J.; Macfarlane, R. J.; Jones, M. R.; Auyeung, E.; Lee, B.; Mirkin, C. A. Stepwise evolution of DNA-

- programmable nanoparticle superlattices. *Angew. Chem., Int. Ed. Engl.* **2013**, *52* (26), 6624–6628.
- (65) Petrosko, S. H.; Coleman, B. D.; Drout, R. J.; Schultz, J. D.; Mirkin, C. A. Spherical nucleic acids: integrating nanotechnology concepts into general chemistry curricula. *J. Chem. Educ.* **2021**, *98* (10), 3090–3099.
- (66) O'Brien, M. N.; Girard, M.; Lin, H. X.; Millan, J. A.; Olvera de la Cruz, M.; Lee, B.; Mirkin, C. A. Exploring the zone of anisotropy and broken symmetries in DNA-mediated nanoparticle crystallization. *Proc. Natl. Acad. Sci. U.S.A.* **2016**, *113* (38), 10485–10490.
- (67) Sun, S.; Yang, S.; Xin, H. L.; Nykypanchuk, D.; Liu, M.; Zhang, H.; Gang, O. Valence-programmable nanoparticle architectures. *Nat. Commun.* **2020**, *11* (1), 2279.
- (68) Young, K. L.; Ross, M. B.; Blaber, M. G.; Rycenga, M.; Jones, M. R.; Zhang, C.; Senesi, A. J.; Lee, B.; Schatz, G. C.; Mirkin, C. A. Using DNA to design plasmonic metamaterials with tunable optical properties. *Adv. Mater.* **2014**, *26* (4), 653–659.
- (69) Zhang, Y.; Pal, S.; Srinivasan, B.; Vo, T.; Kumar, S.; Gang, O. Selective transformations between nanoparticle superlattices via the reprogramming of DNA-mediated interactions. *Nat. Mater.* **2015**, *14* (8), 840–847.
- (70) Maye, M. M.; Kumara, M. T.; Nykypanchuk, D.; Sherman, W. B.; Gang, O. Switching binary states of nanoparticle superlattices and dimer clusters by DNA strands. *Nat. Nanotechnol.* **2010**, *5* (2), 116–120.
- (71) Sun, D.; Tian, Y.; Zhang, Y.; Xu, Z.; Sfeir, M. Y.; Cotlet, M.; Gang, O. Light-harvesting nanoparticle core shell clusters with controllable optical output. *ACS Nano* **2015**, *9* (6), 5657–5665.
- (72) Sun, D.; Gang, O. Binary heterogeneous superlattices assembled from quantum dots and gold nanoparticles with DNA. *J. Am. Chem. Soc.* **2011**, *133* (14), 5252–5254.
- (73) Lin, H.; Lee, S.; Sun, L.; Spellings, M.; Engel, M.; Glotzer, S. C.; Mirkin, C. A. Clathrate colloidal crystals. *Science* **2017**, *355*, 931–935.
- (74) Lu, F.; Yager, K. G.; Zhang, Y.; Xin, H.; Gang, O. Superlattices assembled through shape-induced directional binding. *Nat. Commun.* **2015**, *6*, 6912.
- (75) Ross, M. B.; Ku, J. C.; Vaccarezza, V. M.; Schatz, G. C.; Mirkin, C. A. Nanoscale form dictates mesoscale function in plasmonic DNA-nanoparticle superlattices. *Nat. Nanotechnol.* **2015**, *10* (5), 453–458.
- (76) Sun, L.; Lin, H.; Park, D. J.; Bourgeois, M. R.; Ross, M. B.; Ku, J. C.; Schatz, G. C.; Mirkin, C. A. Polarization-dependent optical response in anisotropic nanoparticle-DNA superlattices. *Nano Lett.* **2017**, *17* (4), 2313–2318.
- (77) Wang, S.; Lee, S.; Du, J. S.; Partridge, B. E.; Cheng, H. F.; Zhou, W.; Dravid, V. P.; Lee, B.; Glotzer, S. C.; Mirkin, C. A. The emergence of valency in colloidal crystals through electron equivalents. *Nat. Mater.* **2022**, *21* (5), 580–587.
- (78) Girard, M.; Wang, S.; Du, J. S.; Das, A.; Huang, Z.; Dravid, V. P.; Lee, B.; Mirkin, C. A.; Olvera de la Cruz, M. Particle analogs of electrons in colloidal crystals. *Science* **2019**, *364*, 1174–1178.
- (79) Cheng, H. F.; Wang, S.; Mirkin, C. A. Electron-equivalent valency through molecularly well-defined multivalent DNA. *J. Am. Chem. Soc.* **2021**, *143* (4), 1752–1757.
- (80) Wang, S.; Du, J. S.; Diercks, N. J.; Zhou, W.; Roth, E. W.; Dravid, V. P.; Mirkin, C. A. Colloidal crystal "alloys". *J. Am. Chem. Soc.* **2019**, *141* (51), 20443–20450.
- (81) Loweth, C. J.; Caldwell, W. B.; Peng, X.; Alivisatos, A. P.; Schultz, P. G. DNA-based assembly of gold nanocrystals. *Angew. Chem., Int. Ed. Engl.* **1999**, *38* (12), 1808–1812.
- (82) Fu, A.; Micheel, C. M.; Cha, J.; Chang, H.; Yang, H.; Alivisatos, A. P. Discrete Nanostructures of quantum dots/Au with DNA. *J. Am. Chem. Soc.* **2004**, *126*, 10832–10833.
- (83) Aldaye, F. A.; Sleiman, H. F. Dynamic DNA templates for discrete gold nanoparticle assemblies: control of geometry, modularity, write/erase and structural switching. *J. Am. Chem. Soc.* **2007**, *129* (14), 4130–4131.
- (84) Mastroianni, A. J.; Claridge, S. A.; Alivisatos, A. P. Pyramidal and chiral groupings of gold nanocrystals assembled using DNA Scaffolds. *J. Am. Chem. Soc.* **2009**, *131* (24), 8455–8459.
- (85) Sonnichsen, C.; Reinhard, B. M.; Liphardt, J.; Alivisatos, A. P. A molecular ruler based on plasmon coupling of single gold and silver nanoparticles. *Nat. Biotechnol.* **2005**, *23* (6), 741–745.
- (86) Zheng, J.; Lukeman, P. S.; Sherman, W. B.; Micheel, C.; Alivisatos, A. P.; Constantinou, P. E.; Seeman, N. C. Metallic nanoparticles used to estimate the structural integrity of DNA motifs. *Biophys. J.* **2008**, *95* (7), 3340–3348.
- (87) Liu, B.; Leontis, N. B.; Seeman, N. C. Bulged 3-arm DNA branched junctions as components for nanoconstruction. *Nanobiology* **1994**, *3*, 177–188.
- (88) He, Y.; Ye, T.; Su, M.; Zhang, C.; Ribbe, A. E.; Jiang, W.; Mao, C. Hierarchical self-assembly of DNA into symmetric supramolecular polyhedra. *Nature* **2008**, *452* (7184), 198–201.
- (89) Wei, B.; Dai, M.; Yin, P. Complex shapes self-assembled from single-stranded DNA tiles. *Nature* **2012**, *485* (7400), 623–626.
- (90) Dey, S.; Fan, C.; Gothelf, K. V.; Li, J.; Lin, C.; Liu, L.; Liu, N.; Nijenhuis, M. A. D.; Saccà, B.; Simmel, F. C.; Yan, H.; Zhan, P. DNA origami. *Nat. Rev. Methods Primers* **2021**, *1* (1), 13.
- (91) Yao, G.; Zhang, F.; Wang, F.; Peng, T.; Liu, H.; Poppleton, E.; Sulc, P.; Jiang, S.; Liu, L.; Gong, C.; Jing, X.; Liu, X.; Wang, L.; Liu, Y.; Fan, C.; Yan, H. Meta-DNA structures. *Nat. Chem.* **2020**, *12* (11), 1067–1075.
- (92) Urban, M. J.; Dutta, P. K.; Wang, P.; Duan, X.; Shen, X.; Ding, B.; Ke, Y.; Liu, N. Plasmonic toroidal metamolecules assembled by DNA origami. *J. Am. Chem. Soc.* **2016**, *138* (17), 5495–5498.
- (93) Kuzyk, A.; Schreiber, R.; Fan, Z.; Pardatscher, G.; Roller, E. M.; Hoge, A.; Simmel, F. C.; Govorov, A. O.; Liedl, T. DNA-based self-assembly of chiral plasmonic nanostructures with tailored optical response. *Nature* **2012**, *483* (7389), 311–314.
- (94) Kuzyk, A.; Schreiber, R.; Zhang, H.; Govorov, A. O.; Liedl, T.; Liu, N. Reconfigurable 3D plasmonic metamolecules. *Nat. Mater.* **2014**, *13* (9), 862–866.
- (95) Tian, Y.; Lhermitte, J. R.; Bai, L.; Vo, T.; Xin, H. L.; Li, H.; Li, R.; Fukuto, M.; Yager, K. G.; Kahn, J. S.; Xiong, Y.; Minevich, B.; Kumar, S. K.; Gang, O. Ordered three-dimensional nanomaterials using DNA-prescribed and valence-controlled material voxels. *Nat. Mater.* **2020**, *19* (7), 789–796.
- (96) Wang, M.; Dai, L.; Duan, J.; Ding, Z.; Wang, P.; Li, Z.; Xing, H.; Tian, Y. Programmable assembly of nano-architectures through designing anisotropic DNA origami Patches. *Angew. Chem., Int. Ed. Engl.* **2020**, *59* (16), 6389–6396.
- (97) Acuna, G. P.; Moller, F. M.; Holzmeister, P.; Beater, S.; Lalkens, B.; Tinnefeld, P. Fluorescence enhancement at docking sites of dna-directed self-assembled nanoantennas. *Science* **2012**, *338* (6106), 506–510.
- (98) Puchkova, A.; Vietz, C.; Pibiri, E.; Wunsch, B.; Sanz Paz, M.; Acuna, G. P.; Tinnefeld, P. DNA origami nanoantennas with over 5000-fold fluorescence enhancement and single-molecule detection at 25  $\mu$ M. *Nano Lett.* **2015**, *15* (12), 8354–8359.
- (99) Thacker, V. V.; Herrmann, L. O.; Sigle, D. O.; Zhang, T.; Liedl, T.; Baumberg, J. J.; Keyser, U. F. DNA origami based assembly of gold nanoparticle dimers for surface-enhanced Raman scattering. *Nat. Commun.* **2014**, *5*, 3448.
- (100) Meyer, T. A.; Zhang, C.; Bao, G.; Ke, Y. Programmable assembly of iron oxide nanoparticles using DNA origami. *Nano Lett.* **2020**, *20* (4), 2799–2805.
- (101) Zhan, P.; Dutta, P. K.; Wang, P.; Song, G.; Dai, M.; Zhao, S. X.; Wang, Z. G.; Yin, P.; Zhang, W.; Ding, B.; Ke, Y. Reconfigurable three-dimensional gold nanorod plasmonic nanostructures organized on DNA origami tripod. *ACS Nano* **2017**, *11* (2), 1172–1179.
- (102) Huang, Y.; Nguyen, M. K.; Natarajan, A. K.; Nguyen, V. H.; Kuzyk, A. A DNA origami-based chiral plasmonic sensing device. *ACS Appl. Mater. Interfaces* **2018**, *10* (51), 44221–44225.
- (103) Funck, T.; Nicoli, F.; Kuzyk, A.; Liedl, T. Sensing picomolar concentrations of RNA using switchable plasmonic chirality. *Angew. Chem., Int. Ed. Engl.* **2018**, *57* (41), 13495–13498.

- (104) Nummelin, S.; Shen, B.; Piskunen, P.; Liu, Q.; Kostianen, M. A.; Linko, V. Robotic DNA nanostructures. *ACS Synth. Biol.* **2020**, *9* (8), 1923–1940.
- (105) Liu, S.; Jiang, Q.; Wang, Y.; Ding, B. Biomedical Applications of DNA-Based Molecular Devices. *Adv. Healthc. Mater.* **2019**, *8* (10), No. e1801658.
- (106) Augspurger, E. E.; Rana, M.; Yigit, M. V. Chemical and biological sensing using hybridization chain reaction. *ACS Sens.* **2018**, *3* (5), 878–902.
- (107) Liu, N.; Liedl, T. DNA-assembled advanced plasmonic architectures. *Chem. Rev.* **2018**, *118* (6), 3032–3053.
- (108) Yin, F.; Mao, X.; Li, M.; Zuo, X. Stimuli-responsive DNA-switchable biointerfaces. *Langmuir* **2018**, *34* (49), 15055–15068.
- (109) Del Grosso, E.; Irmisch, P.; Gentile, S.; Prins, L. J.; Seidel, R.; Ricci, F. Dissipative control over the toehold-mediated DNA strand displacement reaction. *Angew. Chem., Int. Ed. Engl.* **2022**, *61* (23), No. e202201929.
- (110) Increasingly complex DNA assemblies. *Nat. Mater.* **2020**, *19* (7), 689.
- (111) Eiser, E. DNA-nanoparticle crystals: Flip-flop lattices. *Nat. Mater.* **2015**, *14* (8), 751–752.
- (112) Tikhomirov, G.; Hoogland, S.; Lee, P. E.; Fischer, A.; Sargent, E. H.; Kelley, S. O. DNA-based programming of quantum dot valency, self-assembly and luminescence. *Nat. Nanotechnol.* **2011**, *6* (8), 485–490.
- (113) Perez, J. M.; Josephson, L.; O'Loughlin, T.; Hogemann, D.; Weissleder, R. Magnetic relaxation switches capable of sensing molecular interactions. *Nat. Biotechnol.* **2002**, *20* (8), 816–820.
- (114) Li, L.; Xing, H.; Zhang, J.; Lu, Y. Functional DNA molecules enable selective and stimuli-responsive nanoparticles for biomedical applications. *Acc. Chem. Res.* **2019**, *52* (9), 2415–2426.
- (115) Tan, L. H.; Xing, H.; Lu, Y. DNA as a powerful tool for morphology control, spatial positioning, and dynamic assembly of nanoparticles. *Acc. Chem. Res.* **2014**, *47* (6), 1881–1890.
- (116) He, X.; Li, Z.; Chen, M.; Ma, N. DNA-programmed dynamic assembly of quantum dots for molecular computation. *Angew. Chem., Int. Ed. Engl.* **2014**, *53* (52), 14447–14450.
- (117) Josephson, L.; Perez, J. M.; Weissleder, R. Magnetic nanosensors for the detection of oligonucleotide sequences. *Angew. Chem., Int. Ed. Engl.* **2001**, *40* (17), 3204–3206.
- (118) Thaxton, C. S.; Mirkin, C. A. Plasmon coupling measures up. *Nat. Biotechnol.* **2005**, *23* (6), 681–682.
- (119) Lee, K.; Cui, Y.; Lee, L. P.; Irudayaraj, J. Quantitative imaging of single mRNA splice variants in living cells. *Nat. Nanotechnol.* **2014**, *9* (6), 474–480.
- (120) Li, M. X.; Xu, C. H.; Zhang, N.; Qian, G. S.; Zhao, W.; Xu, J. J.; Chen, H. Y. Exploration of the kinetics of toehold-mediated strand displacement via plasmon rulers. *ACS Nano* **2018**, *12* (4), 3341–3350.
- (121) Teng, X.; Dai, Y.; Li, J. Methodological advances of bioanalysis and biochemical targeting of intracellular G-quadruplexes. *Exploration* **2022**, *2* (2), 20210214.
- (122) Abou Assi, H.; Garavis, M.; Gonzalez, C.; Damha, M. J. i-Motif DNA: structural features and significance to cell biology. *Nucleic Acids Res.* **2018**, *46* (16), 8038–8056.
- (123) Tateishi-Karimata, H.; Kawauchi, K.; Sugimoto, N. Destabilization of DNA G-Quadruplexes by chemical environment changes during tumor progression facilitates transcription. *J. Am. Chem. Soc.* **2018**, *140* (2), 642–651.
- (124) Idili, A.; Vallee-Belisle, A.; Ricci, F. Programmable pH-triggered DNA nanoswitches. *J. Am. Chem. Soc.* **2014**, *136* (16), 5836–5839.
- (125) Choi, J.; Kim, S.; Tachikawa, T.; Fujitsuka, M.; Majima, T. pH-induced intramolecular folding dynamics of i-motif DNA. *J. Am. Chem. Soc.* **2011**, *133* (40), 16146–16153.
- (126) He, S.; Ge, Z.; Zuo, X.; Fan, C.; Mao, X. Dynamic regulation of DNA nanostructures by noncanonical nucleic acids. *NPG Asia Mater.* **2021**, *13* (1), 14.
- (127) Zhu, J.; Kim, Y.; Lin, H.; Wang, S.; Mirkin, C. A. pH-responsive nanoparticle superlattices with tunable DNA bonds. *J. Am. Chem. Soc.* **2018**, *140* (15), 5061–5064.
- (128) Han, M. S.; Lytton-Jean, A. K. R.; Mirkin, C. A. A gold nanoparticle based approach for screening triplex DNA binders. *J. Am. Chem. Soc.* **2006**, *128* (15), 4954–4955.
- (129) Chen, F.; Lu, Q.; Huang, L.; Liu, B.; Liu, M.; Zhang, Y.; Liu, J. DNA triplex and quadruplex assembled nanosensors for correlating K<sup>+</sup> and pH in lysosomes. *Angew. Chem., Int. Ed. Engl.* **2021**, *60* (10), 5453–5458.
- (130) Lu, J.; Sun, J.; Li, F.; Wang, J.; Liu, J.; Kim, D.; Fan, C.; Hyeon, T.; Ling, D. Highly sensitive diagnosis of small hepatocellular carcinoma using pH-responsive iron oxide nanocluster assemblies. *J. Am. Chem. Soc.* **2018**, *140* (32), 10071–10074.
- (131) Clever, G. H.; Kaul, C.; Carell, T. DNA–metal base pairs. *Angew. Chem., Int. Ed. Engl.* **2007**, *46* (33), 6226–6236.
- (132) Huang, D.; Niu, C.; Wang, X.; Lv, X.; Zeng, G. Turn-On<sup>†</sup> fluorescent sensor for Hg<sup>2+</sup> based on single-stranded DNA functionalized Mn: CDs/ZnS quantum dots and gold nanoparticles by time-gated mode. *Anal. Chem.* **2013**, *85* (2), 1164–1170.
- (133) Iliuk, A. B.; Hu, L.; Tao, W. A. Aptamer in bioanalytical applications. *Anal. Chem.* **2011**, *83* (12), 4440–4452.
- (134) Song, S.; Wang, L.; Li, J.; Fan, C.; Zhao, J. Aptamer-based biosensors. *Trends Analyt. Chem.* **2008**, *27* (2), 108–117.
- (135) Lee, S. E.; Chen, Q.; Bhat, R.; Petkiewicz, S.; Smith, J. M.; Ferry, V. E.; Correia, A. L.; Alivisatos, A. P.; Bissell, M. J. Reversible aptamer-Au plasmon rulers for secreted single molecules. *Nano Lett.* **2015**, *15* (7), 4564–4570.
- (136) Medley, C. D.; Smith, J. E.; Tang, Z.; Wu, Y.; Bamrungsap, S.; Tan, W. Gold nanoparticle-based colorimetric assay for the direct detection of cancerous Cells. *Anal. Chem.* **2008**, *80* (4), 1067–1072.
- (137) Huang, Y. F.; Sefah, K.; Bamrungsap, S.; Chang, H. T.; Tan, W. Selective photothermal therapy for mixed cancer cells using aptamer-conjugated nanorods. *Anal. Chem.* **2008**, *24* (20), 11860–11865.
- (138) Smith, J. E.; Medley, C. D.; Tang, Z.; Shangguan, D.; Lofton, C.; Tan, W. Aptamer-conjugated nanoparticles for the collection and detection of multiple cancer cells. *Anal. Chem.* **2007**, *79* (8), 3075–3082.
- (139) Herr, J.; Smith, J. E.; Medley, C. D.; Shangguan, D.; Tan, W. Aptamer-conjugated nanoparticles for selective collection and detection of cancer cells. *Anal. Chem.* **2006**, *78* (9), 2918–2924.
- (140) Liu, J.; Lu, Y. Preparation of aptamer-linked gold nanoparticle purple aggregates for colorimetric sensing of analytes. *Nat. Protoc.* **2006**, *1* (1), 246–252.
- (141) Liu, J.; Lu, Y. Non-base pairing DNA provides a new dimension for controlling aptamer-linked nanoparticles and sensors. *J. Am. Chem. Soc.* **2007**, *129* (27), 8634–8643.
- (142) Yue, R.; Zhang, C.; Xu, L.; Wang, Y.; Guan, G.; Lei, L.; Zhang, X.; Song, G. Dual key co-activated nanoplatform for switchable MRI monitoring accurate ferroptosis-based synergistic therapy. *Chem.* **2022**, *8* (7), 1956–1981.
- (143) Seok Kim, Y.; Ahmad Raston, N. H.; Bock Gu, M. Aptamer-based nanobiosensors. *Biosens. Bioelectron.* **2016**, *76*, 2–19.
- (144) Chen, J.; Luo, Z.; Sun, C.; Huang, Z.; Zhou, C.; Yin, S.; Duan, Y.; Li, Y. Research progress of DNA walker and its recent applications in biosensor. *Trends Analyt. Chem.* **2019**, *120*, 115626.
- (145) Yehl, K.; Mugler, A.; Vivek, S.; Liu, Y.; Zhang, Y.; Fan, M.; Weeks, E. R.; Salaita, K. High-speed DNA-based rolling motors powered by RNase H. *Nat. Nanotechnol.* **2016**, *11* (2), 184–190.
- (146) Claridge, S. A.; Mastroianni, A. J.; Au, Y. B.; Liang, H. W.; Micheel, C. M.; Fréchet, J. J. M.; Alivisatos, A. P. Enzymatic ligation creates discrete multinanoparticle building blocks for self-assembly. *J. Am. Chem. Soc.* **2008**, *130* (29), 9598–9605.
- (147) Kanaras, A. G.; Wang, Z.; Bates, A. D.; Cosstick, R.; Brust, M. Towards multistep nanostructure synthesis: programmed enzymatic self-assembly of DNA/Gold systems. *Angew. Chem., Int. Ed. Engl.* **2003**, *42* (2), 191–194.

- (148) Nicewarner Peña, S. R.; Raina, S.; Goodrich, G. P.; Fedoroff, N. V.; Keating, C. D. Hybridization and Enzymatic Extension of Au Nanoparticle-Bound Oligonucleotides. *J. Am. Chem. Soc.* **2002**, *124* (25), 7314–7323.
- (149) Andreadis, J. D.; Chrisey, L. A. Use of immobilized PCR primers to generate covalently immobilized DNAs for in vitro transcription/translation reactions. *Nucleic Acids Res.* **2000**, *28* (2), e5.
- (150) Kanaras, A. G.; Wang, Z.; Brust, M.; Cosstick, R.; Bates, A. D. Enzymatic disassembly of DNA–gold nanostructures. *Small* **2007**, *3* (4), 590–594.
- (151) Kanaras, A. G.; Wang, Z.; Hussain, I.; Brust, M.; Cosstick, R.; Bates, A. D. Site-specific ligation of DNA-modified gold nanoparticles activated by the restriction enzyme Styl. *Small* **2007**, *3* (1), 67–70.
- (152) Yin, P.; Yan, H.; Daniell, X. G.; Turberfield, A. G.; Reif, J. H. A unidirectional DNA walker that moves autonomously along a track. *Angew. Chem., Int. Ed. Engl.* **2004**, *116* (37), 5014–5019.
- (153) Bath, J.; Green, S. J.; Turberfield, A. J. A free-running DNA motor powered by a nicking enzyme. *Angew. Chem., Int. Ed. Engl.* **2005**, *117* (28), 4432–4435.
- (154) Xu, M.; Tang, D. Recent advances in DNA walker machines and their applications coupled with signal amplification strategies: A critical review. *Anal. Chim. Acta* **2021**, *1171*, 338523.
- (155) Wu, N.; Wang, K.; Wang, Y. T.; Chen, M. L.; Chen, X. W.; Yang, T.; Wang, J. H. Three-dimensional DNA nanomachine biosensor by integrating DNA walker and rolling machine cascade amplification for ultrasensitive detection of cancer-related gene. *Anal. Chem.* **2020**, *92* (16), 11111–11118.
- (156) Arndt, G. M.; MacKenzie, K. L. New prospects for targeting telomerase beyond the telomere. *Nat. Rev. Cancer* **2016**, *16* (8), 508–524.
- (157) Roake, C. M.; Artandi, S. E. Regulation of human telomerase in homeostasis and disease. *Nat. Rev. Mol. Cell Biol.* **2020**, *21* (7), 384–397.
- (158) Wang, K.; Shangguan, L.; Liu, Y.; Jiang, L.; Zhang, F.; Wei, Y.; Zhang, Y.; Qi, Z.; Wang, K.; Liu, S. In situ detection and imaging of telomerase activity in cancer cell lines via disassembly of plasmonic core-satellites nanostructured probe. *Anal. Chem.* **2017**, *89* (13), 7262–7268.
- (159) Ma, W.; Fu, P.; Sun, M.; Xu, L.; Kuang, H.; Xu, C. Dual quantification of microRNAs and telomerase in living cells. *J. Am. Chem. Soc.* **2017**, *139* (34), 11752–11759.
- (160) Ran, X.; Wang, Z.; Pu, F.; Ju, E.; Ren, J.; Qu, X. Nucleic acid-driven aggregation-induced emission of Au nanoclusters for visualizing telomerase activity in living cells and in vivo. *Mater. Horiz.* **2021**, *8* (6), 1769–1775.
- (161) Sheng, C.; Zhao, J.; Di, Z.; Huang, Y.; Zhao, Y.; Li, L. Spatially resolved in vivo imaging of inflammation-associated mRNA via enzymatic fluorescence amplification in a molecular beacon. *Nat. Biomed. Eng.* **2022**, *6* (9), 1074–1084.
- (162) Shao, Y.; Zhao, J.; Yuan, J.; Zhao, Y.; Li, L. Organelle-specific photoactivation of DNA nanosensors for precise profiling of subcellular enzymatic activity. *Angew. Chem., Int. Ed. Engl.* **2021**, *60* (16), 8923–8931.
- (163) Xiang, Z.; Zhao, J.; Yi, D.; Di, Z.; Li, L. Peptide nucleic acid (PNA)-guided peptide engineering of an aptamer sensor for protease-triggered molecular imaging. *Angew. Chem., Int. Ed. Engl.* **2021**, *60* (42), 22659–22663.
- (164) McConnell, E. M.; Cozma, I.; Mou, Q.; Brennan, J. D.; Lu, Y.; Li, Y. Biosensing with DNAzymes. *Chem. Soc. Rev.* **2021**, *50* (16), 8954–8994.
- (165) Willner, I.; Shlyahovsky, B.; Zayats, M.; Willner, B. DNAzymes for sensing, nanobiotechnology and logic gate applications. *Chem. Soc. Rev.* **2008**, *37* (6), 1153–1165.
- (166) Liu, J.; Wernette, D. P.; Lu, Y. Proofreading and error removal in a nanomaterial assembly. *Angew. Chem., Int. Ed. Engl.* **2005**, *44* (44), 7290–7293.
- (167) Liu, J.; Lu, Y. A colorimetric lead biosensor using DNAzyme-directed assembly of gold nanoparticles. *J. Am. Chem. Soc.* **2003**, *125* (22), 6642–6643.
- (168) Chen, J.; Pan, J.; Chen, S. A naked-eye colorimetric sensor for Hg<sup>(2+)</sup> monitoring with cascade signal amplification based on target-induced conjunction of split DNAzyme fragments. *Chem. Commun.* **2017**, *53* (73), 10224–10227.
- (169) Mazumdar, D.; Liu, J.; Lu, G.; Zhou, J.; Lu, Y. Easy-to-use dipstick tests for detection of lead in paints using non-cross-linked gold nanoparticle-DNAzyme conjugates. *Chem. Commun.* **2010**, *46* (9), 1416–1418.
- (170) Fang, Z.; Huang, J.; Lie, P.; Xiao, Z.; Ouyang, C.; Wu, Q.; Wu, Y.; Liu, G.; Zeng, L. Lateral flow nucleic acid biosensor for Cu<sup>2+</sup> detection in aqueous solution with high sensitivity and selectivity. *Chem. Commun.* **2010**, *46* (47), 9043–9045.
- (171) Zhang, Y.; Xu, J.; Zhou, S.; Zhu, L.; Lv, X.; Zhang, J.; Zhang, L.; Zhu, P.; Yu, J. DNAzyme-triggered visual and ratiometric electrochemiluminescence dual-readout assay for Pb(II) based on an assembled paper device. *Anal. Chem.* **2020**, *92* (5), 3874–3881.
- (172) Xu, J.; Zhang, Y.; Li, L.; Kong, Q.; Zhang, L.; Ge, S.; Yu, J. Colorimetric and electrochemiluminescence dual-mode sensing of lead ion based on integrated lab-on-paper device. *ACS Appl. Mater. Interfaces* **2018**, *10* (4), 3431–3440.
- (173) Xu, L.; Yin, H.; Ma, W.; Wang, L.; Kuang, H.; Xu, C. MRI biosensor for lead detection based on the DNAzyme-induced catalytic reaction. *J. Phys. Chem. B* **2013**, *117* (46), 14367–14371.
- (174) Yin, H.; Kuang, H.; Liu, L.; Xu, L.; Ma, W.; Wang, L.; Xu, C. A ligation DNAzyme-induced magnetic nanoparticles assembly for ultrasensitive detection of copper ions. *ACS Appl. Mater. Interfaces* **2014**, *6* (7), 4752–4757.
- (175) Ma, L.; Liu, J. Catalytic Nucleic Acids: Biochemistry, Chemical Biology, Biosensors, and Nanotechnology. *iScience* **2020**, *23* (1), 100815.
- (176) Cha, T. G.; Pan, J.; Chen, H.; Salgado, J.; Li, X.; Mao, C.; Choi, J. H. A synthetic DNA motor that transports nanoparticles along carbon nanotubes. *Nat. Nanotechnol.* **2014**, *9* (1), 39–43.
- (177) Xin, L.; Zhou, C.; Duan, X.; Liu, N. A rotary plasmonic nanoclock. *Nat. Commun.* **2019**, *10* (1), 5394.
- (178) Yeh, H. C.; Sharma, J.; Han, J. J.; Martinez, J. S.; Werner, J. H. A DNA–silver nanocluster probe that fluoresces upon hybridization. *Nano Lett.* **2010**, *10* (8), 3106–3110.